



# Spider wasp optimizer: a novel meta-heuristic optimization algorithm

Mohamed Abdel-Basset<sup>1</sup> · Reda Mohamed<sup>1</sup> · Mohammed Jameel<sup>2</sup> ·  
Mohamed Abouhawwash<sup>3,4</sup>

/ Published online: 13 March 2023

This is a U.S. Government work and not under copyright protection in the US; foreign copyright protection may apply 2023

## Abstract

This work presents a new nature-inspired meta-heuristic algorithm named spider wasp optimization (SWO) algorithm, which is based on replicating the hunting, nesting, and mating behaviors of the female spider wasps in nature. This proposed algorithm has various unique updating strategies, making it applicable to a wide range of optimization problems with different exploration and exploitation requirements. The proposed SWO is compared with nine newly published and well-established metaheuristics over four different benchmarks: (1) Standard benchmark, including 23 unimodal and multimodal test functions; (2) test suite of CEC2017, (3) test suite of CEC2020, and (4) test suite of CEC2014 to validate its reliability. Moreover, two classical engineering design problems, namely, welded beam and pressure vessel designs, and parameter estimation of the single-diode, double-diode, and triple-diode photovoltaic models are used to further evaluate the performance of SWO in optimizing real-world optimization problems. Experimental findings demonstrate that SWO is more competitive compared with the state-of-art meta-heuristic methods for four validated benchmarks and superior to all observed real-world optimization problems. Specifically, SWO achieves an overall effective percentage of 78.2% on the standard benchmark, 92.31% on CEC2014, 77.78% on CEC2017, 60% on CEC2020, and 100% on real-world problems. The source code of SWO is publicly available at <https://www.mathworks.com/matlabcentral/fileexchange/126010-spider-wasp-optimizer-swo>.

**Keywords** Spider wasp optimizer · Engineering design problems · Constrained optimization · Stochastic optimization · Metaheuristic

## 1 Introduction

Optimization problems have become prevalent in several fields, such as engineering, medicine, decision making, and agriculture (Sahab et al. 2013). Several traditional methods, also known as deterministic methods, have been presented to overcome such

---

✉ Mohamed Abouhawwash  
abouhaww@msu.edu; saleh1284@mans.edu.eg

Extended author information available on the last page of the article

problems; however, these methods suffer from at least one of those problems: (I) falling into local minima, (II) requiring gradient information, (III) time-consuming, and (IV) not applicable for a wide range of the real-world optimization problems (Sahab et al. 2013; Mirjalili and Lewis 2016). As a result, over the last four decades (roughly from 1980 to the present), modern stochastic techniques known as meta-heuristic algorithms (MAs) have been presented to deal with those problems (Glover and Kochenberger 2006; Bianchi et al. 2009; Yang 2012; Sahab et al. 2013; Yang et al. 2013).

Meta-heuristic algorithms typically imitate biological or physical phenomena, also known as nature-inspired MAs. MAs can be partitioned into four main categories: physics-based, evolution-based, swarm-based, and human-based. The first category mainly simulates the physics rules to propose MAs known as physics-based MAs; some of which are Henry gas solubility optimization (Hashim et al. 2019), equilibrium optimizer (EO) (Faramarzi et al. 2020a), gravitational local search algorithm (Webster and Bernhard 2003), multi-verse optimizer (Mirjalili et al. 2016), simulated annealing (Kirkpatrick et al. 1983), charged system search (Kaveh and Talatahari 2010), big-bang big-crunch (Erol and Eksin 2006), central force optimization (Formato 2007), curved space optimization (Moghaddam et al. 2012), galaxy-based search algorithm (Shah-Hosseini 2011), ray optimization (Kaveh and Khayatazad 2012), small-world optimization algorithm (Du et al. 2006), electromagnetism-like algorithm (Birbil and Fang 2003), intelligent water drops algorithm (Shah-Hosseini 2009), river formation dynamics algorithm (Rabanal et al. 2007), space gravitational algorithm (Hsiao, et al. 2005), particle collision algorithm (Sacco and Oliveira 2005), integrated radiation algorithm (Chuang and Jiang 2007), gravitational interactions optimization (Flores et al. 2011), ion motion algorithm (Javidy et al. 2015), and artificial physics algorithm (Xie et al. 2009). The second category called evolution-based MAs simulates the process of natural evolution in nature; some of the prevalent algorithms in this class are genetic algorithm (Holland 1992), evolutionary programming (Yao et al. 1999), evolution strategy (Alavi and Henderson 1981), genetic programming (GP) (Koza and Koza 1992), and differential evolution (Price 2013).

The third category known as swarm-based MAs simulates the social behaviors of the swarm intelligence in animals and birds. This category includes several well-established and newly published optimization algorithms. Examples under this category are as follows: slime mould algorithm (SMA) (Li et al. 2020), whale optimization algorithm (WOA) (Mirjalili and Lewis 2016), marine predators algorithm (MPA) (Faramarzi et al. 2020b), salp swarm algorithm (Mirjalili et al. 2017), particle swarm optimization (Kennedy and Eberhart 1995), Wasp Swarm Optimization (Pinto et al. 2007), Grey wolf optimizer (GWO) (Mirjalili et al. 2014), Bat algorithm (Yang and Gandomi 2012), cuckoo search algorithm (Gandomi et al. 2013), Cat optimization algorithm (Chu et al. 2006), chicken swarm optimization (Meng 2014), artificial gorilla troops optimizer (GTO) (Abdollahzadeh et al. 2021a), Horse herd optimization algorithm (MiarNaeimi et al. 2021), red fox optimization algorithm (RFO) (Połap and Woźniak 2021), ant colony optimization (Dorigo et al. 2006), Krill herd algorithm (Bolaji et al. 2016), elephant herding optimization (Wang et al. 2015), jellyfish search algorithm (Chou and Truong 2021), and Donkey and smuggler optimization algorithm (Shamsaldin et al. 2019).

The last category is human-based MAs, which are inspired by the social behaviors of humans in their life; some of which are teaching–learning-based optimization (Rao et al. 2011), past present future (Naik and Satapathy 2021), soccer league competition (Moosavian and Roodsari 2014), exchange market algorithm (Ghorbani and Babaei 2014), socio evolution and learning optimization algorithm (Kumar et al. 2018), brain storm

optimization (Shi 2011), bus transportation algorithm (Bodaghi and Samieefar 2019), and political optimizer (Askari et al. 2020).

In this work, we introduce a new nature-inspired swarm-based meta-heuristic algorithm for stochastic optimization, namely, spider wasp optimizer (SWO), which is based on replicating the hunting, nesting, and mating behaviors of female spider wasps in nature. The proposed SWO involves four operators that simulate searching for the spider, following and escaping the dropped spider, nesting the paralyzed spider, and mating behavior to lay an egg of the female spider wasps. It is assessed using four different benchmarks: Twenty-three standard test functions, CEC2014, CEC2017, and CEC2020 to analyze its exploration, exploitation, local optima avoidance, and convergence speed. The experimental results show that SWO is the most effective compared to nine state-of-the-art optimization algorithms. Further validation and comparison have been done using two classical engineering design problems (welded beam design (WBD) and pressure vessel design), and the parameter estimation problem for photovoltaic models. The experimental outcomes demonstrated the efficiency of SWO in addressing real-world optimization problems. The main contributions of this paper are listed as follows:

- Simulating hunting, nesting, and mating behaviors of female spider wasps in a newly-proposed stochastic algorithm, namely spider wasp optimizer (SWO), to tackle the continuous optimization problems.
- Assessing SWO using several mathematical benchmarks and real-life optimization problems to show its efficacy.
- SWO is being compared to several optimization algorithms, which are divided into two groups: highly-cited and well-studied algorithms, and recently published algorithms.
- The experimental findings affirm that SWO is a powerful alternative stochastic algorithm for several optimization problems.

The next sections of this article are organized as follows. Section 2 describes the spider wasps in nature. Section 3 presents the proposed spider wasp optimization (SWO) algorithm. Sections 4 and 5 present and discuss the experimental findings of three mathematical benchmarks (CEC2017, CEC2014, and 23 standard test functions), and five real-world optimization problems: WBD; pressure vessel design; estimation of five unknown parameters for SDM, estimation of seven unknown parameters for DDM, and estimation of five unknown parameters for TDM. Section 6 provides the key findings concluded from this study. Section 7 provides the conclusion and future perspectives.

## 2 Spider wasp in the nature: originality

Spider wasps (Pompilidae) are one of the largest aculeate wasps in Hymenoptera and are widespread in large areas of the world, but they are mostly common in tropical areas (Pitts et al. 2006; Loktionov et al. 2019). The family Pompilidae has approximately 5000 described species grouped into 254 genera and five subfamilies in the world (Aguiar, et al. 2013; Waichert et al. 2015; Wahis et al. 2018). Spider wasps are solitary predator insects that utilize the spider as an optimal food source for their offspring. Their names originate from their preferred prey and their unique hunting behavior. This solitary wasp species is characterized by slender bodies and spiny legs (Pitts et al. 2006). There are a few vividly colored species of this wasp species, but often they are blue or black, sometimes with a

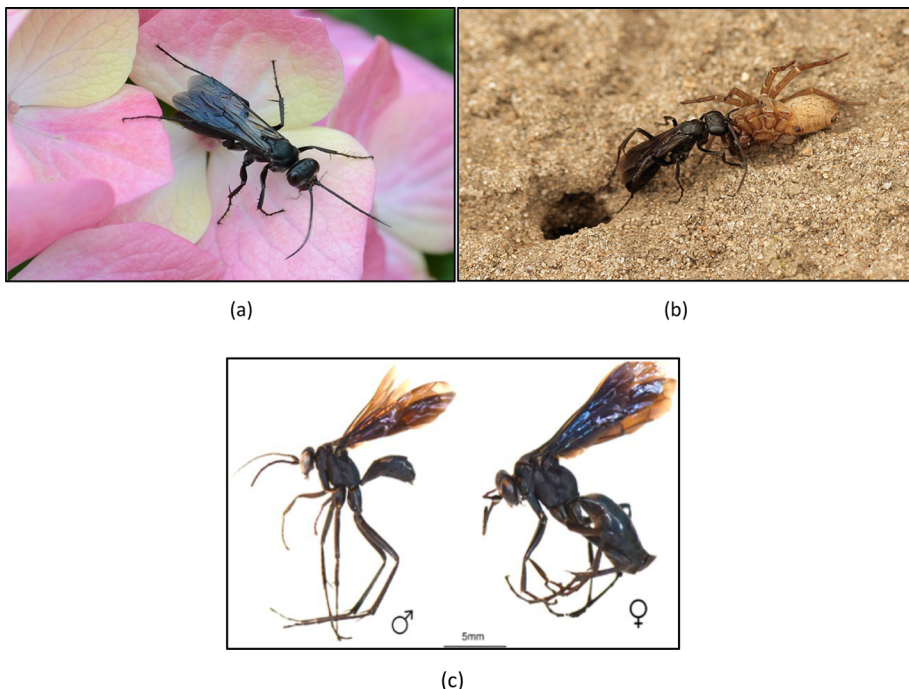


**Fig. 1** **a** Spider wasp female; **b** spider wasp female drags a paralyzed spider toward her open burrow; **c** male and female spider wasps. Note the female's significantly greater body size

metallic shine (Waichert et al. 2015). Fig. 1a shows a species of a female wasp (with black color). They usually feed on flower nectar or search for prey on the ground. Female spider wasps hunt spiders to provide enough food for their larvae. The largest species in the Pompilidae family is called the “tarantula hawks” due to their unique predatory behavior on a fierce host, the tarantula (Pitts et al. 2006).

Female spider wasps have unique hunting and nesting behaviors, which are utilized to search for their adequate prey (spider) and nests for feeding and to lay their eggs. In terms of hunting behavior, female spider wasps use a variety of foraging strategies to randomly search for their prey in the surrounding environments. Female wasps start randomly searching for spiders that serve as hosts for their larvae. They walk on the ground or foliage with wings vibrating and antennae in constant motion, in addition to making brief trips. Once a suitable host spider is found and located, the female spider wasp begins to chase it within the hub of its web by running or flying, subduing it with one or more venomous bites in the underside of its cephalothorax (Kurczewski and Edwards 2012; Starr 2012). However, the spider might drop from its web to the ground and is followed by the female wasps to paralyze it for feeding their larva (Rayor 1996). The sting is inserted close to a significant nerve center, which affects the host's ability to move. The prey does not die but remains in a state of permanent paralysis (Punzo 1994). Once the spider acquiesced, the spider wasps begin to explore the surface of the spider with its antennae (Punzo 1994; Kurczewski and Edwards 2012). Then, the wasps pull the paralyzed spider into the pre-prepared nest, grasping a pedipalp with their mandibles (Shimizu 1992; Kurczewski and Edwards 2012). Fig. 1(b), which is taken from Kurczewski and Edwards (2012) shows a spider wasp

dragging its prey (spider) on a pre-prepared burrow. It digs burrows with its forelegs by scraping soil backward (Evans and Shimizu 1996). A female spider wasp lays one egg on the spider's abdomen and then closes the nest (Nishimoto et al. 2021). After a few days, the wasp's egg hatches and begins to consume the edible parts of the host (spider) using its mandibles (Pitts et al. 2006; Aguiar, et al. 2013). The wasp larva develops on the paralyzed spider for several days, goes through various stages of development until it becomes an adult, and emerges from the nest after a few weeks (Kurczewski and Edwards 2012). The size of the host spider should be sufficient to provide food for the developing wasp larvae.

Spider wasps have a variety of nesting behaviors, such as digging and building cells in the soil or making nests of mud in leaves or rocks (Grissell et al. 1997; Nieves-Aldrey et al. 2006). Others use pre-existing nests or cavities, such as spider's (prey) nests or beetle holes (Nieves-Aldrey et al. 2006; Shimizu et al. 2010; Carvalho-Filho et al. 2015). Based on the size of the prey spider, female spider wasps can determine the sex of their progeny (King 1988; Starr 2012; Benamu et al. 2020). A female spider wasp can choose the sex of her progeny at the time of laying eggs using the haplodiploid sex-determination system (found in all hymenopterans) (Starr 2012; Benamu et al. 2020). This notion means that mothers should lay mostly unfertile eggs (males) on small hosts and fertile eggs (females) on large hosts, if growing on large hosts (spiders) imparts more reproductive success on females than males (Charnov et al. 1981; Opp and Luck 1986; Benamu et al. 2020). Thus, the size of the males is smaller compared with that of the females. Fig. 1c, which is taken from Kurczewski and Edwards (2012), shows the size of the male and female spider wasps.

Several studies have shown a positive correlation between the host-spider and the spider wasp sizes (Endo and Endo 1994; Kurczewski and Edwards 2012; Kurczewski and Kieran 2015). These studies concluded that the spider wasp size significantly increased with increasing host weight. Studies have also shown a noticeable increase in the size of female spider wasps compared with males (Evans and Shimizu 1996; Nishimoto et al. 2021). This increase is because mothers choose a large host for females rather than males. Therefore, the host's weight is essential for the growth and survival of the larvae.

Other studies have shown that some eggs fail to grow (Punzo 1994; Auko et al. 2013), such as Starr (Starr 2012), which evaluated the reproductive success of a set of spider wasps and determined that over 85% survive to adulthood; this study was based on 700 nests. The spider wasp's failure to survive is due to the lack of a spider of sufficient size to feed the larvae (Auko et al. 2013). A small host will not simply provide enough food for the wasp larva. Several external reasons lead to burrow and larval growth failure, including building nests in a dry area, particularly on rocks; Another insect discovers the nest and strives to destroy it while eating the larva with its host (Kurczewski and Edwards 2012; Shimizu et al. 2012). Other unknown causes exist (Shimizu et al. 2012; Nishimoto et al. 2021).

### 3 Spider wasp optimizer: SWO

This work introduces a new optimization algorithm inspired by hunting and nesting behaviors and the obligate brood parasitism for some species of wasps by laying a single egg in the abdomen of each spider. At first, female spider wasps explore the surrounding environments for suitable spiders, paralyzing and dragging them to pre-prepared suitable nests; this behavior represents the first inspiration of our proposed algorithm: SWO. After finding the suitable prey and nests and dragging them in these nests, they lay an egg on the

abdomen of spider and close the nest. The proposed algorithm (SWO) randomly distributes a number of female wasps within the search space. Then, each one will explore the search space in constant motion in search of a spider suitable for the sex of its progeny as determined by the haplodiploid sex-determination system found in all hymenopterans according to their hunting behaviors known as hunting and following behaviors. After finding suitable spiders, the female spider wasps will forage them within their web hub and search the ground six times for the spiders dropped from the web (Rayor 1996). Afterward, the female wasps will attack the prey and try to paralyze it to be dragged to the pre-prepared nest. Then, she closes the nest after laying an egg in the spider's abdomen. In brief, the behaviors of the wasps simulated in this work are listed below:

- Searching behavior: This behavior seeks for the prey at the start of the optimization to find the spider suitable for the larval growth.
- Following and escaping behavior: After finding the prey/spiders, they may attempt to flee the orb of the hub. Hence, the female wasp follows them, paralyzing and dragging the most suitable one.
- Nesting behavior: this will simulate the manner of dragging the prey to the nests with a size appropriate for the prey and egg.
- Mating behavior: this behavior simulates the properties of the offspring produced by hatching the egg using the uniform crossover operator between the male and the female wasps with a specific probability known as crossover rate (CR).

The mathematical model of those behaviors, in addition to more detailed description of them, will be presented in the next subsection.

### 3.1 Generation of the initial population

In the proposed algorithm, each spider-wasp (female) represents a solution in the current generation and can be encoded in the  $D$ -dimension vector by the following expressions:

$$\overrightarrow{SW} = [x_1, x_2, x_3, \dots, x_D] \quad (1)$$

A set of  $N$  vectors can be randomly generated between the pre-specified upper initial parameter bound  $\vec{H}$  and the lower initial parameter bound  $\vec{L}$ , as follows:

$$SW_{Pop} = \begin{bmatrix} SW_{1,1} & SW_{1,2} & \dots & SW_{1,D} \\ SW_{2,1} & SW_{2,2} & \dots & SW_{2,D} \\ \vdots & \vdots & \vdots & \vdots \\ SW_{N,1} & SW_{N,2} & \dots & SW_{N,D} \end{bmatrix} \quad (2)$$

where  $SW_{Pop}$  is the initial population of spider wasps. The following equation can be used to randomly generate any solution in the search space:

$$\overrightarrow{SW}_i' = \vec{L} + \vec{r} \times (\vec{H} - \vec{L}) \quad (3)$$

where  $t$  denotes the generation index;  $i$  indicates the population index ( $i = 1, 2, \dots, N$ ); and  $\vec{r}$  is a vector of  $D$ -dimension randomly initialized numbers between 0 and 1. Next, the

spider wasp behaviors will be mathematically simulated to introduce a novel metaheuristic algorithm for tackling the optimization problems. The behaviors are as follows:

- Hunting and nesting behavior
- Mating behavior

### 3.2 Hunting and nesting behavior

The female spider wasps start their trip by searching for the spider/prey that will feed their larvae. Their search is randomly performed within the search space to find the most suitable prey, and this is referred to as the searching or exploration stage. Afterward, it will encircle the prey and chase it by running or flying. This stage is called the encircling and chasing phase. Finally, in the last stage, the spider wasp will drag the paralyzed spider into the pre-prepared nest to lay the egg over its abdomen.

#### 3.2.1 Searching stage (exploration)

This stage simulates the behavior of the female wasps in finding the most relevant spiders to feed their larvae. In this stage, the female wasp randomly explores the search space with a constant step, as previously described, to find the spider that will be suitable for their offspring. This behavior is modeled, as shown in Eq. (4), which updates the current position of each female with a constant motion at each generation  $t$  to simulate the exploration behavior of the female wasp.

$$\overline{SW}_i^{t+1} = \overline{SW}_i^t + \mu_1 * \left( \overline{SW}_a^t - \overline{SW}_b^t \right) \quad (4)$$

where  $a$  and  $b$  are two indices selected at random from the population to determine the exploration direction, followed by the female wasps; and  $\mu_1$  is employed to determine the constant motion through the current direction using the following formula:

$$\mu_1 = |rn| * r_1 \quad (5)$$

where  $r_1$  is a number randomly generated at the interval of zero and one, and  $rn$  is also a random number but generated using the normal distribution.

Female wasps sometimes lose track of the dropped spider from the orb; hence, they search the entire region surrounded by the exact spot where this spider dropped. According to this behavior, another equation with different exploration methods has been constructed to enable the proposed algorithm to explore the regions around the dropped spider with a small step size different from that of Eq. (4). This equation is also based on updating the current female wasp with a constant motion at each generation based on the position of a female wasp randomly chosen from the population to represent the position of the dropped spider. This equation is described below:

$$\overline{SW}_i^{t+1} = \overline{SW}_c^t + \mu_2 * \left( \vec{L} + \vec{r}_2 * \left( \vec{H} - \vec{L} \right) \right) \quad (6)$$

$$\mu_2 = B * \cos(2\pi l) \quad (7)$$

$$B = \frac{1}{1 + e^l} \quad (8)$$

where  $c$  is an index randomly selected from the population, and  $l$  is a number randomly generated between 1 and  $-2$ .

In Fig. 2, the values of  $\mu_1$  and  $\mu_2$  within 100 generations are independently repeated twice and shown to highlight the effect of each on the optimization process. As depicted in Fig. 2a, after a while (highlighted by a red ellipse),  $\mu_1$  generates a huge number reaching 2, and this will take the current position to a far position for exploring the regions there, possibly avoiding the local minima problem. In normal mode,  $\mu_1$  generates values ranging between 0 and 0.8 with a mean of 0.4, as shown by the black line depicted in this figure. Those values help in gradually exploring the search space to reach the most promising area that involves the near-optimal solution. Figure 2b depicts the values of  $\mu_2$  and shows that those values range between  $-0.8$  and  $0.8$  and that the direction of search is determined based on the value of  $\mu_2$ ; this will help in avoiding the wrong direction that might be determined by Eq. (4). Equations (4) and (6) complement each other to explore the search space and locate the most promising regions. Finally, the preference between Eqs. (4) and (6) to generate the next position for the female wasp is randomly achieved as described below:

$$\overline{SW}_i^{t+1} = \begin{cases} \text{Eq. (4)} & r_3 < r_4, \\ \text{Eq. (6)} & \text{otherwise}, \end{cases} \quad (9)$$

where  $r_3$  and  $r_4$  are two random numbers in  $[0, 1]$ .

### 3.2.2 Following and escaping stage (exploration and exploitation)

After finding the prey, the spider wasp attempts to attack them in the hub of the web; however, they drop on the ground to escape. It follows the dropped spiders to paralyze and drag them to the pre-prepared nests. In other circumstances, the spider loses track of the spiders dropping from the hub, which means that the wasp tries to catch the spider while also fleeing. This behavior simulates two trends: the first one is the wasp hunting spiders to trap them; in this case, Eq. (10) is applied to update the location of the spider wasp

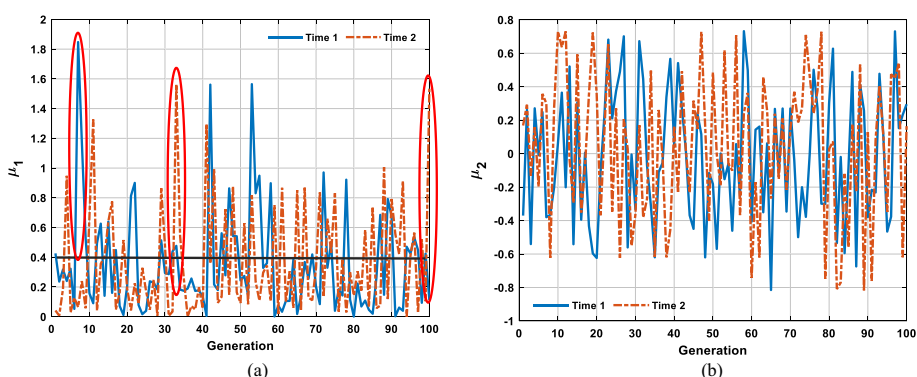


**Fig. 2** Comparison between  $\mu_1$  and  $\mu_2$  motions

to follow the prey; and the second behavior simulates evading the wasps by designing a distance factor to increase the distance between them as the current iteration increases; hence, the prey might hide in some regions far from the wasp. The first trend, which is mathematically expressed in the following equation, simulates chasing wasps to spiders to catch them, where the distance between the prey and the wasps is initially small and may increase or decrease according to the speed of the wasp and prey. In this trend, we propose a mathematical model that simulates two cases: (1) the wasp faster than the spider (prey)  $C > 0.5$  and (2) the prey faster than the wasp  $C < 0.5$ , where  $C$  is a distance controlling factor to determine the speed of the wasp and starts with a speed of two and linearly reduces to zero. In this case, the wasp moves faster than the prey, simulating the spider escaping from the wasp, and the distance between the wasp and spider increases. Hence, when the wasp moves with a speed less than 0.5, the change rates in its position are particularly small that it cannot reach the prey.

$$\overline{SW}_i^{t+1} = \overline{SW}_i^t + C * \left| 2 * \vec{r}_5 * \overline{SW}_a^t - \overline{SW}_i^t \right| \quad (10)$$

$$C = \left( 2 - 2 * \left( \frac{t}{t_{max}} \right) \right) * r_6 \quad (11)$$

where  $a$  is an index randomly selected from the population;  $t$  and  $t_{max}$  indicate the current and maximum evaluation, respectively;  $\vec{r}_5$  is a vector that represents the values randomly generated in the interval  $[0, 1]$ ; and  $r_6$  is a random number in the interval  $[0, 1]$ .

When a spider flees from the female wasp, the distance between the female wasp and the spider gradually increases. This stage is initially exploitation. Exploitation is converted into exploration with the increase in the distance. This behavior is simulated using the following formula:

$$\overline{SW}_i^{t+1} = \overline{SW}_i^t * \overline{vc} \quad (12)$$

where  $\overline{vc}$  is a vector generated between  $k$  and  $-k$  according to the normal distribution. Accordingly,  $k$  is generated using Eq. (13) to gradually increase the distance between the female wasp and the spider.

$$k = 1 - \left( \frac{t}{t_{max}} \right) \quad (13)$$

The tradeoff between those two trends is randomly achieved, as shown in the following equation:

$$\overline{SW}_i^{t+1} = \begin{cases} Eq.(10)r_3 < r_4 \\ Eq.(12)otherwise \end{cases} \quad (14)$$

At the start of the optimization process, all the wasps will apply the exploration mechanism to globally search the domain of the optimization problems to find the promising region that might contain the near-optimal solution. The algorithm will use following

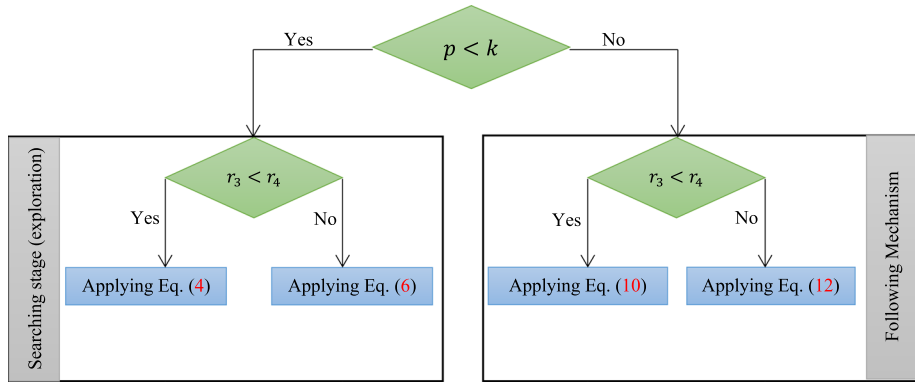


**Fig. 3** Tradeoff between the searching stage and the following and escaping mechanism

and escaping mechanism to explore and exploit the areas around the current wasps during the iteration pass in the hope of avoiding becoming stuck in local minima. Finally, the exchange between the searching stage and the following mechanism is adjusted according to the following formula:

$$\overrightarrow{SW}_i^{t+1} = \begin{cases} Eq.(9)p < k \\ Eq.(14)otherwise \end{cases} \quad (15)$$

where  $p$  is a random number in  $[0, 1]$ . The tradeoff between searching and the following mechanism is pictured in Fig. 3.

### 3.2.3 Nesting behavior (exploitation)

The wasp females pull the paralyzed spider into the pre-prepared nest. Spider wasps have numerous nesting behaviors, such as digging and building cells in the soil, building nests of mud in leaves or rocks, or using the pre-existing nests or cavities, such as spider's (prey) nests or beetle holes. These behaviors are simulated in our proposed algorithm with two different equations because spider wasps have various nesting behaviors. The first equation is based on pulling the spider toward the region that contains the most suitable spider and deeming it the best place to build the nest for placing the paralyzed spider and laying egg over its abdomen. This first equation is described as follows:

$$\overrightarrow{SW}_i^{t+1} = \overrightarrow{SW}^* + \cos(2\pi l) * (\overrightarrow{SW}^* - \overrightarrow{SW}_i^t) \quad (16)$$

where  $SW^*$  represents the best-so-far solution. The second equation will build the nest within the position of a female spider randomly selected from the population using an additional step size to avoid building two nests within the same position. This equation is designed as follows:

$$\overrightarrow{SW}_i^{t+1} = \overrightarrow{SW}_a^t + r_3 * |\gamma| * (\overrightarrow{SW}_a^t - \overrightarrow{SW}_i^t) + (1 - r_3) * \overrightarrow{U} * (\overrightarrow{SW}_b^t - \overrightarrow{SW}_c^t) \quad (17)$$

where  $r_3$  is a random number created in the interval  $[0, 1]$ ;  $\gamma$  is a number generated according to the levy flight;  $a$ ,  $b$ , and  $c$  are indices of three solutions randomly selected from the population;  $\overline{U}$  is a binary vector used to determine when a step size is applied to avert building two nests at the same position; and  $\overline{U}$  is assigned according to the following formula:

$$\overline{U} = \begin{cases} 1 & \vec{r}_4 > \vec{r}_5 \\ 0 & \text{otherwise} \end{cases} \quad (18)$$

where  $\vec{r}_4$  and  $\vec{r}_5$  are two vectors that represent the random values in the interval  $[0, 1]$ . Equations (16) and (17) are randomly exchanged according to the following formula:

$$\overline{SW}_i^{t+1} = \begin{cases} Eq.(16) & r_3 < r_4 \\ Eq.(17) & \text{otherwise} \end{cases} \quad (19)$$

Finally, the tradeoff among hunting and nesting behaviors are achieved by Eq. (20) and depicted in Fig. 4, where all the spider wasps will search for their relevant spider at the start of the optimization process. Then, the wasps will pull their suitable wasps into the pre-prepared nests.

$$\overline{SW}_i^{t+1} = \begin{cases} Eq.(15) & i < N * k \\ Eq.(19) & \text{otherwise} \end{cases} \quad (20)$$

### 3.3 Mating behavior

The mating of wasps is taken into consideration in the proposed algorithm. One of the main characteristics of spider wasps is their ability to determine gender. Gender is determined based on the size of the host in which an egg is laid. Males are represented by small spider wasps, while females are indicated by large wasps (Fig. 1c).

In the introduced approach, each spider wasp represents a possible solution in the current generation, and the spider wasp egg represents the newly generated potential solution in that generation. The new solutions/spider wasp eggs are generated according to the following equation:

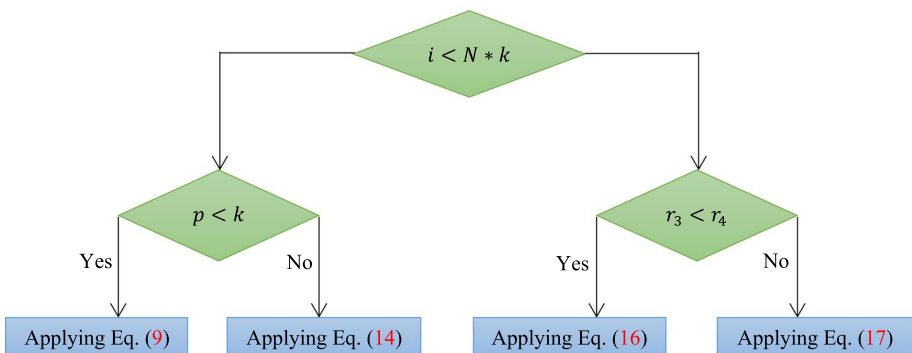


**Fig. 4** Flowchart of the hunting and nesting behaviors in SWO

$$SW_i^{t+1} = \text{Crossover}(SW_i^t, SW_m^t, CR) \quad (21)$$

where *Crossover* indicates the uniform crossover operator that is applied between solutions  $SW_i^t$  and  $SW_m^t$  with a probability known as crossover rate (CR);  $SW_m^t$  and  $SW_i^t$  are two vectors that represent the male and female spider wasps, respectively. The male spider wasp is generated in our proposed algorithm to be different from the female wasps according to the following formula:

$$\overline{SW}_m^{t+1} = \overline{SW}_i^t + e^l * |\beta| * \vec{v}_1 + (1 - e^l) * |\beta_1| * \vec{v}_2 \quad (22)$$

where  $\beta$  and  $\beta_1$  are two numbers randomly generated according to the normal distribution,  $e$  is the exponential constant, and  $\vec{v}_1$  and  $\vec{v}_2$  are generated according to the following formula:

$$\vec{v}_1 = \begin{cases} \vec{x}_a - \vec{x}_i & f(\vec{x}_a) < f(\vec{x}_i) \\ \vec{x}_i - \vec{x}_a & \text{otherwise} \end{cases} \quad (23)$$

$$\vec{v}_2 = \begin{cases} \vec{x}_b - \vec{x}_c & f(\vec{x}_b) < f(\vec{x}_c) \\ \vec{x}_c - \vec{x}_b & \text{otherwise} \end{cases} \quad (24)$$

where  $a$ ,  $b$ , and  $c$  are indices of three solutions randomly selected from the population, such that  $a \neq i \neq b \neq c$ . Crossover is used to recombine the genetic material in two-parent spider wasps to produce an offspring (egg) that shares the characteristics of their parents. The tradeoff between hunting and mating behaviors is based on a predefined factor known as tradeoff rate (TR). This rate is discussed in detail in the experiments.

### 3.4 Population reduction and memory saving

After the female spider lays an egg on the abdomen of the host, it closes the nest and leaves the nest site inconspicuous. This notion means that the role of this female in the optimization process is nearly completed, and delegating their function evaluations to the other wasps for the remainder of the optimization process might help in reaching better results. During the iteration run, some wasps in the population will be terminated to provide more function evaluations to the other wasps while also reducing population diversity to accelerate the convergence speed toward the near-optimal solution. In each evaluation of the whole function evaluations, the length of the new population will be updated using the following formula:

$$N = N_{min} + (N - N_{min}) \times k \quad (25)$$

where  $N_{min}$  indicates the minimum number of the population employed to avoid being stuck into local minima within the different stages of the optimization process. Finally, memory saving is conducted by our proposed algorithm to preserve the best-spider position obtained by each wasp to be updated in the next generation. In brief, each solution obtained by each wasp is compared with its equivalent in the prior generation, and the current one is replaced by the new one if it is more fitted. The pseudo-code of SWO is listed in Algorithm 1.

**Algorithm 1** The proposed SWO

**Input:**  $N$ ,  $N_{min}$ ,  $CR$ ,  $TR$ ,  $t_{max}$

**Output:**  $\overrightarrow{SW}^*$

1. Initialize  $N$  female wasps,  $\overrightarrow{SW}_i$  ( $i = 1, 2, \dots, N$ ), using Eq. (3)
2. Evaluate each  $\overrightarrow{SW}_i$  and finding the one with the best fitness in  $\overrightarrow{SW}^*$
3.  $t = 1$ ; //the current function evaluation
4. **while** ( $t < t_{max}$ )
5.      $r_6$ : generating a random number between 0 and 1
6.     **if** ( $r_6 < TR$ ) %% Hunting and Nesting behaviors
7.         **for**  $i=1:N$
8.             *Applying Fig. 4*
9.             *Compute  $f(\overrightarrow{SW}_i)$*
10.              $t=t+1$ ;
11.         **End for**
12.         **Else** %% Mating Behavior
13.         **for**  $i=1:N$
14.             *Applying Eq. (21)*
15.              $t=t+1$ ;
16.         **End for**
17.         **End if**
18.         *Applying Memory Saving*
19.         Updating  $N$  using Eq. (25)
20. **End while**

### 3.5 Time complexity

This subsection will focus on the big-O time complexity, which will be tailored to demonstrate the speedup of the introduced approach. For starters, the following are the primary elements that significantly impact the proposed algorithm's speedup:

- The population size:  $N$ .
- The number of dimensions:  $D$
- The maximum function evaluation:  $t_{max}$ .

In brief, the time complexity formula of the proposed SWO is designed as follows:

$$T(SWO) = T(\text{Hunting and Nesting behaviors}) + T(\text{Mating Behavior}) \quad (26)$$

Broadly speaking, the time complexity of both hunting and Nesting behaviors and mating behavior mainly relies on the former three factors and that is aggregated in big-O according to Algorithm 1 as follows:

$$T(SWO) = O(t_{max}DN) + O(t_{max}DN) \quad (27)$$

From Eq. (27), both hunting and Nesting behaviors and mating behavior have the same growth rate in big-O. Therefore, the time complexity of the introduced SWO in the worst

case is of  $O(t_{max}DN)$ . Both  $N$  and  $t_{max}$  factors, being associated with the metaheuristic algorithms, will eventually stabilise at a fixed value, as further increases in either will have no discernible effect on the metaheuristics' efficiency. For this reason, we will refer to both of them as constants. Hence, the time taken by SWO is directly proportional to  $D$ ; therefore, it will be labeled as  $O(D)$  in big-O.

## 4 Numerical experiment

The introduced algorithm (SWO) is first assessed using 23 standard test functions that are widely utilized in the literature and divided into six unimodal ( $F_1 - F_6$ ), seven multimodal ( $F_7 - F_{13}$ ), and ten fixed dimension multimodal test functions ( $F_{14} - F_{23}$ ). The unimodal test function is utilized to evaluate the exploitation capability of the proposed algorithm, while its exploration ability is observed by the multimodal test function. In our experiments, the unimodal and multimodal test functions have been experimented in 50 dimensions. The fixed dimension test functions are herein employed to test the exploration capability of SWO in low dimensions. The mathematical models and characteristics of some of those 23 standard test functions in addition to their topologies are found in Appendix A, and the rest are carefully described in Faramarzi et al. (2020b). The maximum number of function evaluations for SWO and other rival algorithms is 50,000 to ensure a fair comparison during our experiments.

The introduced SWO is extensively compared with nine existing optimization algorithms selected based on two classes in order to demonstrate its effectiveness. These classes are as follows: (1) the first class is comprised of some of the more recently-published algorithms, such as the slime mould algorithm (SMA) (Li et al. 2020), artificial gorilla troops optimizer (GTO) (Abdollahzadeh et al. 2021a), equilibrium optimizer (EO) (Faramarzi et al. 2020a), African vultures optimization algorithm (AVOA) (Abdollahzadeh et al. 2021b), marine predators algorithm (MPA) (Faramarzi et al. 2020b), and red Fox optimizer (RFO) (Połap and Woźniak 2021); and the second class includes some of the highly-cited and well-studied metaheuristic optimization algorithms: whale optimization algorithm (WOA) (Mirjalili and Lewis 2016), grey wolf optimizer (GWO) (Mirjalili et al. 2014), and sine cosine algorithm (SCA) (Mirjalili 2016). All of these competing algorithms were developed in an effort to solve the global optimization problem that was investigated and solved in this study. Because of this, we conducted our experiments using the controlling parameter values that were recommended by the authors of these competing algorithms as set to Table 1. Each of those algorithms was run 25 independent times, and the obtained fitness values have been categorized as Best, Average (Ave), Worst, Standard deviation (Std), and Rank. The Wilcoxon rank-sum test was also utilized to determine how statistically different the obtained fitness values by the introduced algorithm from those of competitors.

The introduced algorithm has three parameters that have to be effectively estimated to maximize its performance; those parameters are the minimum population size  $N_{m,TR}$ , and  $CR$ . Numerous experiments have been run to determine the most effective value for each parameter. Parameter  $TR$  is checked using three test functions:  $F_1$ ,  $F_2$ , and  $F_{12}$  with values ranging between 0 and 1.0. SWO was run 30 times on each investigated value for this parameter and the obtained fitness values are depicted in Fig. 5. Increasing the value for this parameter improves the performance of the introduced algorithm for unimodal test functions. Meanwhile, decreasing the value down to 0.08 improves its performance for the multimodal test functions. Thus, the introduced algorithm has a high ability to be used to

**Table 1** Parameter settings for the proposed and rival algorithms

Algorithms	Parameters	Value	Algorithms	Parameters	Value
GWO (2014)	Convergence constant $a$ $N$	Decreases Linearly from 2 to 0 30	SMA (2020)	$z$ $N$	0.03 30
WOA (2017)	Convergence constant $a$ Spiral factor $b$ $N$	Decreases Linearly from 2 to 0 1 30	GTO (2021)	$p$ $Beta$ $w$ $N$	0.03 3 8 30
SCA (2016)	Convergence constant $a$ $N$	2 25	AVOA (2021)	Alpha ( $L_1$ ) Beta ( $L_2$ ) Gamma ( $w$ ) $P_1$ $P_2$ $P_3$ $N$	0.8 0.2 2.5 0.6 0.4 0.6 30
EO (2020)	$a_1$ $a_2$ $V$ $GP$ $N$	2 1 1 0.5 30	RFO (2021)	$N$	100
MPA (2020)	$FADs$ $P$ $N$	0.2 0.5 25	SWO	$TR$ $CR$ $N_m$ $N$	0.3 0.2 20 100

a variety of optimization problems by adapting the parameter  $TR$ . This parameter was set a value of 0.3 in the trials undertaken for this research. Figure 6 shows that the best value for the parameter  $CR$  is 0.2 under two standard test functions:  $F_6$  and  $F_{12}$ .  $N_m$  and  $N$  are set to 20 and 100 after conducting several experiments, respectively.

The proposed and rival algorithms have been implemented by MATLAB R2019a over a device with the following capabilities:

- Central processing unit (CPU): Intel(R) Core (TM) i7-4700MQ CPU @ 2.40 GHz
- The installed random-access memory is 32 GB
- Equipped with 64-bit Windows 10 Pro.

#### 4.1 Exploitation analysis of SWO

The unimodal test functions have only one global solution and involve no local minima; thus, they could be utilized to assess the exploitation capability of SWO. In this section, extensive experiments have been conducted to observe the performance of MPA and rival methods over the standard unimodal test functions ( $F_1 - F_7$ ). Table 2 presents the outcomes of MPA and rival methods for those test functions, which shows the superiority of MPA for  $F_6$  against all the rival methods and its competitiveness with SMA, RFO, AVOA, WOA, and GTO for F1, F2, F3, and F4. However, SWO could not outperform AVOA for F5 and F7. The experiments demonstrated that the introduced algorithm is superior to

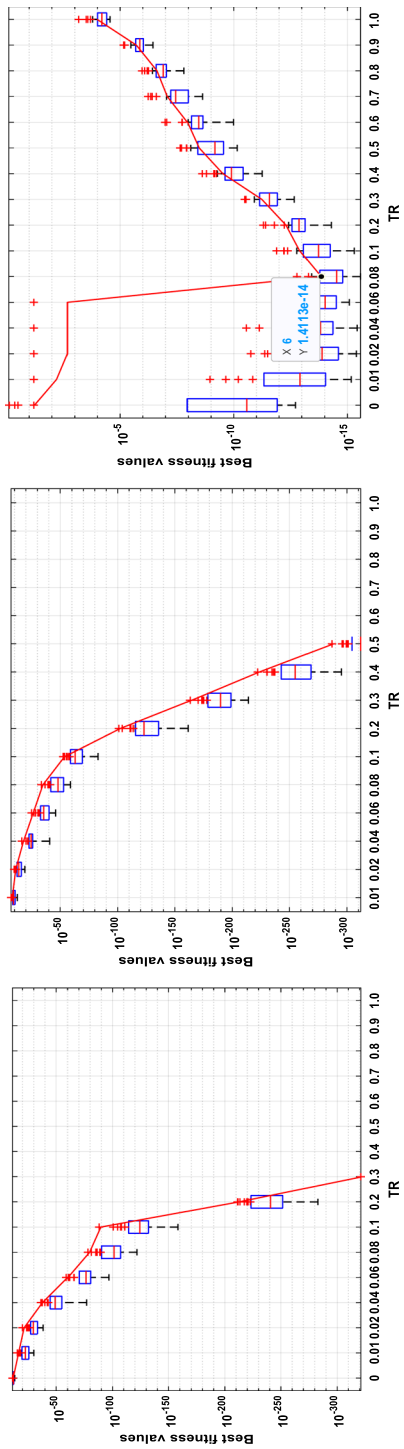


**Fig. 5** Tuning of parameter  $TR$

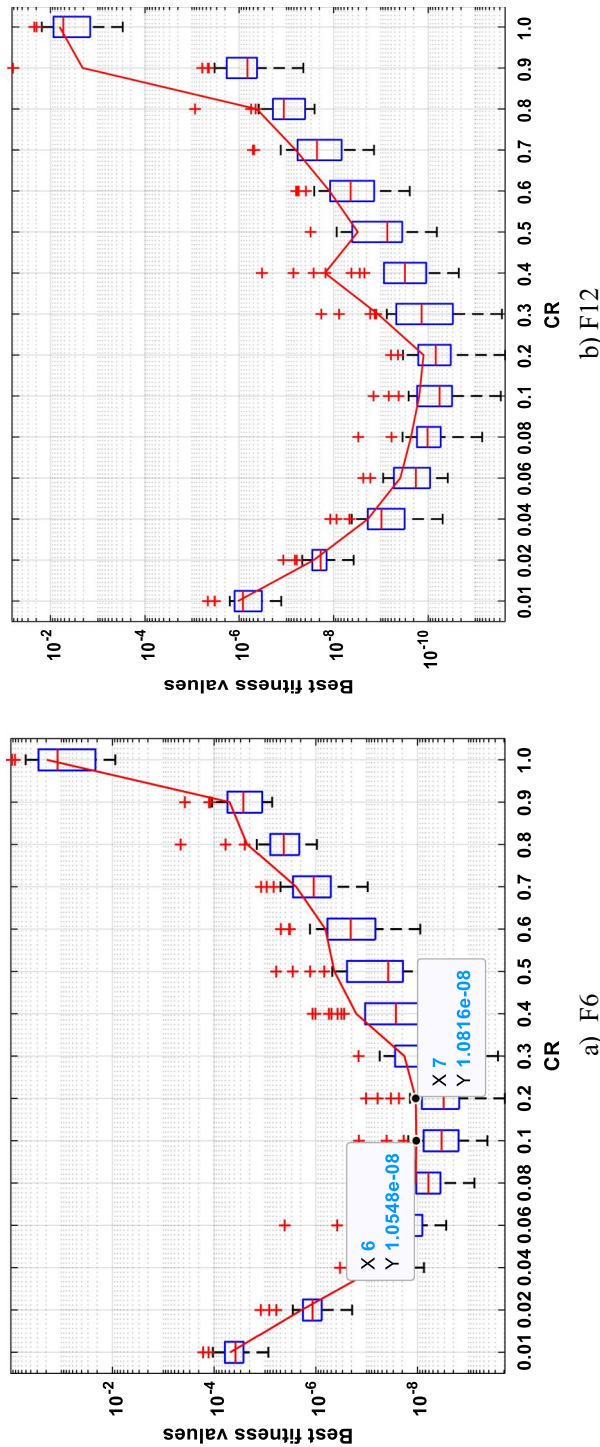


Fig. 6 Tuning of parameter  $CR$

**Table 2** Outcomes for unimodal test functions

Function	SMA	RFO	AVOA	EO	WOA	GTO	MPA	SCA	GWO	SWO	
Unimodal F1	Best	<b>0</b>	<b>0</b>	<b>0</b>	1.44E - 128	<b>0</b>	<b>0</b>	8.07E - 9	0.0004	1.14E - 77 <b>0</b>	
	Ave	<b>0</b>	<b>0</b>	<b>0</b>	2.08E - 121	<b>0</b>	<b>0</b>	1.02E - 46	1.4885	2.94E - 75 <b>0</b>	
	Worst	<b>0</b>	<b>0</b>	<b>0</b>	5.21E - 120	<b>0</b>	<b>0</b>	1.31E - 45	8.4224	1.67E - 74 <b>0</b>	
F2	Best	<b>0</b>	<b>0</b>	<b>0</b>	2.19E - 74	<b>0</b>	<b>0</b>	4.28E - 29	3.57E - 09	1.61E - 45 <b>0</b>	
	Ave	<b>0</b>	<b>0</b>	<b>0</b>	1.10E - 71	<b>0</b>	<b>0</b>	2.50E - 26	1.16E - 04	1.91E - 44 <b>0</b>	
	Worst	<b>0</b>	<b>0</b>	<b>0</b>	1.41E - 70	<b>0</b>	<b>0</b>	1.70E - 25	2.71E - 03	9.91E - 44 <b>0</b>	
F3	Best	<b>0</b>	<b>0</b>	<b>0</b>	8.24E - 32	27.759.93	<b>0</b>	7.88E - 12	6175.3276	4.04E - 20 <b>0</b>	
	Ave	<b>0</b>	<b>0</b>	<b>0</b>	2.83E - 22	74.492.76	<b>0</b>	1.44E - 06	23.633.4117	2.02E-13 <b>0</b>	
	Worst	<b>0</b>	<b>0</b>	<b>0</b>	5.43E - 21	119.068.4	<b>0</b>	1.10E - 05	42.208.8060	3.43E - 12 <b>0</b>	
F4	Best	<b>0</b>	<b>0</b>	<b>0</b>	1.08E - 31	1.338063	<b>0</b>	2.80E - 18	24.2336	1.29E - 17 <b>0</b>	
	Ave	<b>0</b>	<b>0</b>	<b>0</b>	3.48E - 26	56.77122	<b>0</b>	1.07E - 17	49.3951	3.35E - 16 <b>0</b>	
	Worst	<b>0</b>	<b>0</b>	<b>0</b>	4.81E - 25	92.59815	<b>0</b>	3.52E - 17	64.2788	2.85E - 15 <b>0</b>	
F5	Best	0.0068	48.5603	<b>3.15E - 07</b>	4.35E+01	4.63E+01	2.10E - 07	43.7083	97.5119	45.6776	41.0645
	Ave	0.5826	48.6449	<b>2.18E - 06</b>	4.39E+01	4.71E+01	0.000856	44.6895	613.397.8707	47.1442	41.8867
	Worst	1.8499	48.8323	<b>7.90E - 06</b>	4.42E+01	4.86E+01	0.012769	48.2749	7.513.906.2946	48.6181	43.0970
F6	Best	5.52E - 04	1.56E - 02	3.90E - 09	6.78E - 09	2.27E - 02	2.30E - 08	5.55E - 08	8.5987	1.25092	<b>1.12E - 10</b>
	Ave	3.15E - 03	2.60E - 02	8.71E - 09	1.13E - 07	6.58E - 02	2.46E - 07	0.036228	17.6723	2.4603	<b>3.08E - 09</b>
	Worst	5.45E - 03	3.98E - 02	2.94E - 08	9.92E - 07	1.51E - 01	1.31E - 06	0.178769	149.9560	3.5094	<b>2.13E - 08</b>
F7	Best	6.56E - 06	2.54E - 06	<b>5.70E - 07</b>	1.37E - 04	1.34E - 05	9.25E - 06	3.42E - 04	2.51E - 02	3.42E - 04	6.97E - 05
	Ave	6.56E - 05	4.37E - 05	<b>3.54E - 05</b>	4.86E - 04	1.26E - 03	6.34E - 05	7.95E - 04	1.88E - 01	7.14E - 04	7.03E - 04
	Worst	2.09E - 04	1.43E - 04	<b>1.18E - 04</b>	8.62E - 04	6.31E - 03	1.55E - 04	1.49E - 03	9.54E - 01	1.42E - 03	1.66E - 03

Bold values mark the best values

most newly published algorithms and competitive with the others in terms of exploitation capability.

## 4.2 Exploration analysis of SWO

This section assesses the performance of the SWO and rival methods for the multimodal test functions, which have been widely utilized for evaluating the exploration capability because they involve many local minima. The local minima are directly proportional to the number of dimensions. In this section, the algorithm performance is evaluated in high and low (fixed) dimension multimodal test functions, specifically F8–F23. Table 3 illustrates the results of SWO and other rival methods on these test functions. According to this table, the SWO outperforms all methods on F12 and F13, but its performance is comparable to that of high-performance optimization algorithms, such as SMA, RFO, AVOA, GTO, EO, and MPA. The rank metric must be used to check the rank of each algorithm on each test function to fully assess the performance of each algorithm because SWO is competitive with some rival methods on various test functions. The average of this metric shown in Table 3 on each test function is computed on all test functions and displayed in Fig. 7, which confirms that SWO is the best with a value of 1.19, and SCA is the worst with nearly 5. Fig. 8 has been presented to report the average of Std on all test functions to show how far each algorithm could reach almost similar outcomes in all independent times. This figure shows that SWO is more stable with a value of 2377.

Finally, the Wilcoxon rank-sum statistical test under a significant level of 5% is utilized to investigate the significant difference between the outcomes of SWO and those of the competitors. Table 4 shows the p-values of the Wilcoxon rank-sum statistical test. This table illustrates that the results of SWO are significantly different from those of the other

**Table 3** Results for multimodal test functions

	Function	SMA	RFO	AVOA	EO	WOA	GTO	MPA	SCA	GWO	SWO
Multimodal (High-dimensional)	F8	Best Ave Worst	<b>-2.09E+04</b> <b>-2.09E+04</b> <b>-2.09E+04</b>	-1.44E+04 -1.19E+04 -1.03E+04	<b>-2.09E+04</b> -2.06E+04 -1.79E+04	-1.51E+04 -1.34E+04 -1.12E+04	<b>-2.09E+04</b> -2.00E+04 -1.50E+04	-1.75E+04 -1.48E+04 -2.09E+04	-6.37E+03 -5.26E+03 -4.72E+03	-1.18E+04 -1.85E+04 -8.15E+03	-1.97E+04 -1.85E+04 -1.65E+04
	Rank	1	7	2	6	3	1	5	9	8	4
	F9	Best Ave Worst	0.000 0.000 0.000	0.000 0.000 0.000	0.000 0.000 0.000	0.000 0.000 0.000	0.000 0.000 0.000	0.000 0.000 0.000	1.735E-05	<b>0.000</b>	<b>0.000</b>
	Rank	1	1	1	1	1	1	1	2	1	1
F10	Best	8.88E-16	8.88E-16	8.88E-16	4.441E-15	<b>8.88E-16</b>	8.88E-16	<b>8.88E-16</b>	3.72E-03	1.51E-14	8.88E-16
	Ave	8.88E-16	8.88E-16	8.88E-16	4.441E-15	3.30E-15	<b>8.88E-16</b>	4.30E-15	1.47E+01	1.77E-14	8.88E-16
	Worst	8.88E-16	8.88E-16	8.88E-16	4.441E-15	7.99E-15	<b>8.88E-16</b>	4.44E-15	2.05E+01	2.93E-14	8.88E-16
	Rank	1	1	1	4	2	1	3	6	5	1
F11	Best	0.000	0.000	0.000	0.000	0.000	0.000	0.000	<b>0.000</b>	<b>0.000</b>	<b>0.000</b>
	Ave	0.000	0.000	0.000	0.000	0.000	0.000	0.000	0.633	0.001	<b>0.000</b>
	Worst	0.000	0.000	0.000	0.000	0.000	0.000	0.000	1.130	0.018	<b>0.000</b>
	Rank	1	1	1	1	1	1	1	3	2	1
F12	Best	8.83E-07	1.79E-04	7.02E-11	1.07E-10	7.29E-04	9.57E-13	7.24E-09	7.13E-01	3.16E-02	5.96E-14
	Ave	1.10E-03	2.67E-04	1.98E-10	3.54E-09	3.30E-03	1.94E-08	8.36E-04	3.55E+05	7.61E-02	1.42E-11
	Worst	5.57E-03	4.26E-04	4.38E-10	2.50E-08	2.01E-02	9.20E-08	3.07E-03	4.17E+06	1.44E-01	2.01E-10
	Rank	7	5	2	3	8	4	6	10	9	1
F13	Best	3.21E-05	3.86E-03	9.80E-11	4.62E-8	5.86E-02	1.90E-0	2.48E-03	7.66E+00	9.77E-01	1.74E-11
	Ave	1.27E-03	1.99E+00	1.58E-09	5.28E-02	2.51E-01	7.33E-04	1.71E-01	9.41E+05	1.83E+00	1.11E-09
	Worst	4.21E-03	4.99E+00	<b>4.77E-09</b>	2.07E-01	6.36E-01	1.10E-02	4.75E-01	9.73E+06	2.64E+00	1.29E-08
	Rank	4	8	2	5	7	3	6	10	9	1

**Table 3** (continued)

	Function	SMA	RFO	AVOA	EO	WOA	GTO	MPA	SCA	GWO	SWO
Multimodal (Fixed-dimensional)	F14	Best <b>0.998</b>	0.998	<b>0.998</b>	<b>0.998</b>	0.998	<b>0.998</b>	<b>0.998</b>	0.998	0.998	<b>0.998</b>
	Ave	<b>0.998</b>	9.346	<b>0.998</b>	<b>0.998</b>	2.408	<b>0.998</b>	<b>0.998</b>	1.157	4.599	<b>0.998</b>
	Worst	<b>0.998</b>	12.671	<b>0.998</b>	<b>0.998</b>	10.763	<b>0.998</b>	<b>0.998</b>	2.982	12.671	<b>0.998</b>
F15	Rank	<b>1</b>	5	<b>1</b>	<b>1</b>	3	<b>1</b>	<b>1</b>	2	4	<b>1</b>
	Best	<b>0.000308</b>	<b>0.000307</b>	<b>0.000307</b>	<b>0.000307</b>	0.000310	<b>0.000307</b>	<b>0.000307</b>	0.000382	0.000307	<b>0.000307</b>
	Ave	<b>0.000408</b>	0.000345	0.000308	0.000381	0.000780	0.000454	<b>0.000307</b>	0.000877	0.007601	<b>0.000307</b>
F16	Worst	0.000773	0.001236	0.000324	0.001223	0.002252	0.001223	<b>0.000307</b>	0.001405	0.020363	<b>0.000307</b>
	Rank	5	3	2	4	7	6	<b>1</b>	8	9	<b>1</b>
	Best	<b>-1.031628</b>	-1.031628	<b>-1.031628</b>	<b>-1.031628</b>	-1.031628	<b>-1.031628</b>	<b>-1.031628</b>	-1.031628	-1.031628	<b>-1.031628</b>
F17	Ave	<b>-1.031628</b>	-0.998982	<b>-1.031628</b>	<b>-1.031628</b>	-1.031628	<b>-1.031628</b>	<b>-1.031628</b>	-1.031617	-1.031628	<b>-1.031628</b>
	Worst	<b>-1.031628</b>	-0.215464	<b>-1.031628</b>	<b>-1.031628</b>	-1.031628	<b>-1.031628</b>	<b>-1.031628</b>	-1.031575	-1.031628	<b>-1.031628</b>
	Rank	<b>1</b>	3	<b>1</b>	<b>1</b>	<b>1</b>	<b>1</b>	<b>1</b>	2	<b>1</b>	<b>1</b>
F18	Best	0.3979	<b>0.3979</b>	0.3979	<b>0.3979</b>	0.3979	<b>0.3979</b>	<b>0.3979</b>	0.3979	0.3979	0.3979
	Ave	0.3979	<b>0.3979</b>	0.3979	<b>0.3979</b>	0.3979	<b>0.3979</b>	<b>0.3979</b>	0.3979	0.3979	0.3979
	Worst	0.3979	0.3979	<b>0.3979</b>	<b>0.3979</b>	0.3979	<b>0.3979</b>	<b>0.3979</b>	0.4013	0.3981	0.3979
F19	Rank	<b>1</b>	1	<b>1</b>	<b>1</b>	<b>1</b>	<b>1</b>	<b>1</b>	<b>1</b>	<b>1</b>	<b>1</b>
	Best	<b>3.0000</b>	3.0000	<b>3.0000</b>	<b>3.0000</b>	<b>3.0000</b>	<b>3.0000</b>	<b>3.0000</b>	<b>3.0000</b>	<b>3.0000</b>	<b>3.0000</b>
	Ave	<b>3.0000</b>	3.0000	<b>3.0000</b>	<b>3.0000</b>	<b>3.0000</b>	<b>3.0000</b>	<b>3.0000</b>	<b>3.0000</b>	<b>3.0000</b>	<b>3.0000</b>
Worst	Worst	<b>3.0000</b>	3.0000	<b>3.0000</b>	<b>3.0000</b>	3.0001	<b>3.0000</b>	<b>3.0000</b>	<b>3.0000</b>	<b>3.0000</b>	<b>3.0000</b>
	Rank	<b>1</b>	1	<b>1</b>	<b>1</b>	2	<b>1</b>	<b>1</b>	<b>1</b>	<b>1</b>	<b>1</b>
	Best	<b>-3.8628</b>	-3.8628	<b>-3.8628</b>	<b>-3.8628</b>	-3.8628	<b>-3.8628</b>	<b>-3.8628</b>	-3.8620	-3.8628	<b>-3.8628</b>
Worst	Ave	<b>-3.8628</b>	-3.8628	<b>-3.8628</b>	<b>-3.8628</b>	-3.8628	<b>-3.8628</b>	<b>-3.8628</b>	-3.8553	-3.8618	<b>-3.8628</b>
	Worst	<b>-3.8628</b>	-3.8628	<b>-3.8628</b>	<b>-3.8628</b>	-3.8549	<b>-3.8628</b>	<b>-3.8628</b>	-3.8536	-3.8550	<b>-3.8628</b>
	Rank	<b>1</b>	1	<b>1</b>	<b>1</b>	3	<b>1</b>	<b>1</b>	4	2	<b>1</b>

**Table 3** (continued)

	Function	SMA	RFO	AVOA	EO	WOA	GTO	MPA	SCA	GWO	SWO
F20	Best	<b>-3.3220</b>	-3.3220	-3.3220	-3.3220	-3.3220	-3.3220	-3.3220	-3.1923	-3.3220	-3.3220
	Ave	-3.2364	-3.2694	-3.2649	-3.3030	-3.2150	-3.2649	-3.3220	-2.9323	-3.2688	-3.3220
	Worst	-3.2031	-3.2008	-3.2031	-3.2031	-3.0807	-3.2031	-3.3220	-2.2591	-3.0830	-3.3220
F21	Rank	6	4	5	3	8	2	1	9	7	1
	Best	<b>-10.1532</b>	-10.1532	-10.1532	-10.1531	-10.1532	-10.1532	-10.1532	<b>-5.0190</b>	-10.1532	-10.1532
	Ave	-10.1532	-5.6706	-10.1532	-9.7454	-8.3754	-10.1532	-10.1532	-2.1305	-10.1532	-10.1532
F22	Worst	-10.1531	-5.0552	-10.1532	-5.0552	-0.8820	-10.1532	-10.1532	-0.4965	-10.1531	-10.1532
	Rank	2	5	1	3	4	1	1	6	2	1
	Best	<b>-10.4029</b>	-10.4029	-10.4029	<b>-10.4029</b>	<b>-10.4029</b>	-10.4029	-10.4029	-8.3939	-10.4029	-10.4029
F23	Ave	<b>-10.4029</b>	-5.9398	-10.4029	-10.4029	-9.7517	-10.4029	-10.4029	-3.3778	-10.1903	-10.4029
	Worst	-10.4028	-5.0877	-10.4029	<b>-10.4029</b>	-5.0877	-10.4029	-10.4029	-0.5240	-5.0877	-10.4029
	Rank	1	4	1	1	3	1	1	5	2	1
	Best	<b>-10.5364</b>	-10.5364	<b>-10.5364</b>	<b>-10.5364</b>	-10.5363	-10.5364	-10.5364	-9.9512	<b>-10.5364</b>	-10.5364
	Ave	-10.5364	-5.5630	-10.5364	-10.3201	-10.0995	-10.5364	-10.5364	-5.1616	-9.9974	-10.5364
	Worst	-10.5363	-5.1285	-10.5364	-5.1285	-2.8065	-10.5364	-10.5364	-0.9437	-2.4217	-10.5364
	Rank	1	5	1	2	3	1	1	6	4	1

Bold values mark the best values

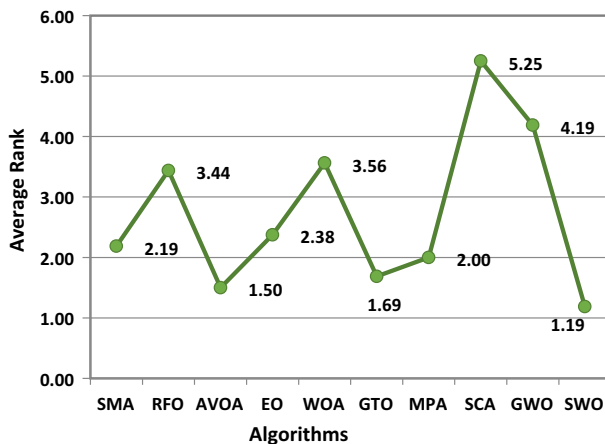


**Fig. 7** Depiction of the average rank on all test functions

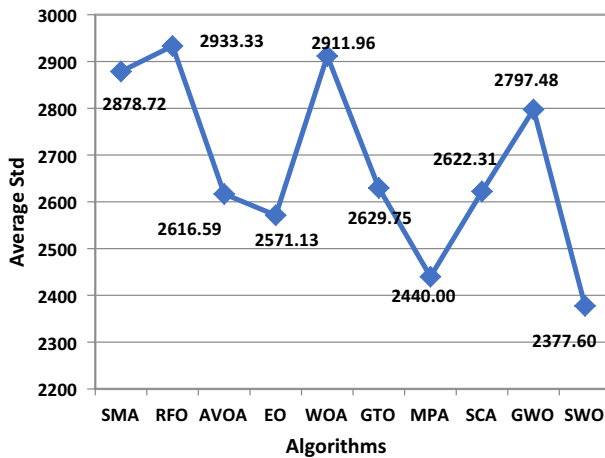


**Fig. 8** Depiction of the average Std on all test functions

methods because the p-value is less than 0.05 for most test functions; hence, the alternative hypothesis is accepted. SWO's exploration is strong due to the various optimization phases confined to hunting and mating behaviors.

#### 4.3 Performance evaluation on the CEC-2017 test suite

Some test functions of one of the most recent and challenging benchmarks on numerical optimization competitions known as CEC-2017 are selected to further observe the performance of the suggested algorithm (Awad et al. 2017). This benchmark contains 30 test functions, which are unimodal, multimodal, hybrid, and composition, to strongly challenge the previously proposed and the newly-proposed optimizers. In our experiments, 18 test functions different from multimodal, unimodal, hybrid, and composition are selected to

**Table 4** p-Values of the Wilcoxon rank-sum test for F8-F23

	Function	SMA	RFO	AVOA	EO	WOA	GTO	MPA	SCA	GWO
Wilcoxon	F8	<b>1.416E-09</b>	<b>1.416E-09</b>	<b>6.184E-08</b>	<b>1.416E-09</b>	<b>3.899E-05</b>	<b>1.416E-09</b>	<b>2.286E-09</b>	<b>1.416E-09</b>	<b>1.416E-09</b>
Rank-sum	F9	NaN	9.728E-11	NaN						
test	F10	NaN	NaN	NaN	<b>2.772E-12</b>	<b>1.607E-05</b>	NaN	1.891E-11	9.728E-11	<b>4.054E-11</b>
	F11	NaN	9.728E-11	1.615E-01						
	F12	<b>1.416E-09</b>	<b>1.416E-09</b>	<b>8.281E-09</b>	<b>1.507E-09</b>	<b>1.416E-09</b>	<b>8.281E-09</b>	<b>1.416E-09</b>	<b>1.416E-09</b>	<b>1.416E-09</b>
	F13	<b>3.020E-11</b>	<b>3.020E-11</b>	<b>7.739E-06</b>	<b>3.020E-11</b>	<b>3.020E-11</b>	<b>3.474E-10</b>	<b>3.020E-11</b>	<b>3.020E-11</b>	<b>3.020E-11</b>
	F14	<b>9.581E-11</b>	<b>9.592E-11</b>	<b>2.425E-06</b>	<b>8.100E-02</b>	<b>9.728E-11</b>	NaN	<b>8.100E-02</b>	<b>9.728E-11</b>	<b>9.728E-11</b>
	F15	<b>1.387E-09</b>	<b>1.387E-09</b>	<b>1.387E-09</b>	<b>1.387E-09</b>	<b>1.387E-09</b>	<b>6.332E-01</b>	<b>3.500E-01</b>	<b>1.387E-09</b>	<b>1.387E-09</b>
	F16	<b>7.543E-10</b>	<b>7.543E-10</b>	<b>2.481E-01</b>	<b>2.292E-02</b>	<b>7.533E-10</b>	<b>1.199E-03</b>	<b>3.673E-03</b>	<b>7.543E-10</b>	<b>7.543E-10</b>
	F17	<b>1.376E-10</b>	<b>1.376E-10</b>	<b>3.371E-01</b>	<b>3.371E-01</b>	<b>1.376E-10</b>	<b>3.371E-01</b>	<b>3.371E-01</b>	<b>1.376E-10</b>	<b>1.376E-10</b>
	F18	<b>7.357E-10</b>	<b>7.364E-10</b>	<b>7.364E-10</b>	<b>8.259E-04</b>	<b>7.364E-10</b>	<b>1.898E-03</b>	<b>2.083E-05</b>	<b>7.364E-10</b>	<b>7.364E-10</b>
	F19	<b>9.728E-11</b>	<b>9.728E-11</b>	<b>2.089E-10</b>	<b>2.063E-02</b>	<b>9.728E-11</b>	<b>1.094E-03</b>	NaN	<b>9.728E-11</b>	<b>9.728E-11</b>
	F20	<b>1.376E-10</b>	<b>1.376E-10</b>	<b>1.525E-09</b>	<b>1.330E-02</b>	<b>1.376E-10</b>	<b>7.786E-05</b>	<b>3.371E-01</b>	<b>1.376E-10</b>	<b>1.376E-10</b>
	F21	<b>7.188E-10</b>	<b>7.188E-10</b>	<b>1.623E-06</b>	<b>4.875E-02</b>	<b>7.188E-10</b>	<b>9.489E-02</b>	<b>2.671E-01</b>	<b>7.188E-10</b>	<b>7.188E-10</b>
	F22	<b>6.683E-10</b>	<b>6.683E-10</b>	<b>5.983E-06</b>	<b>6.425E-01</b>	<b>6.683E-10</b>	<b>5.754E-01</b>	<b>1.094E-03</b>	<b>6.683E-10</b>	<b>6.683E-10</b>
	F23	<b>2.469E-10</b>	<b>2.469E-10</b>	<b>2.306E-09</b>	<b>6.120E-03</b>	<b>2.469E-10</b>	<b>2.593E-01</b>	<b>4.760E-06</b>	<b>2.469E-10</b>	<b>2.469E-10</b>

Bold values indicate accepting the alternative hypothesis

**Table 5** Results of CEC-2017 test functions

	Function	SMA	RFO	AVOA	EO	WOA	GTO	MPA	SCA	GWO	SVO	
Unimodal	F24	Best	325,000	113,000	101,000	<b>100,000</b>	1,62E+05	<b>100,000</b>	4,52E+08	159,000	<b>100,000</b>	
		Ave	8240,000	2580,000	2130,000	1570,000	1,93E+06	1700,000	<b>100,000</b>	7,11E+08	3,68E+07	
		Worst	1.270E+04	1.270E+04	5630,000	4540,000	1,18E+07	6410,000	<b>100,000</b>	1,08E+09	5,08E+08	
		Rank	6	5	4	2	7	3	<b>1</b>	9	8	
F25	Best	<b>300,000</b>	<b>300,000</b>	<b>300,000</b>	<b>300,000</b>	<b>300,000</b>	<b>467,016</b>	<b>300,000</b>	<b>300,000</b>	<b>685,242</b>	<b>300,789</b>	
		Ave	300,002	583,405	<b>300,000</b>	<b>300,000</b>	1348,816	<b>300,000</b>	<b>300,000</b>	1436,061	1820,693	<b>300,000</b>
		Worst	300,013	5504,466	<b>300,000</b>	<b>300,000</b>	6716,626	<b>300,000</b>	<b>300,000</b>	2378,661	5996,603	<b>300,000</b>
		Rank	2	3	<b>1</b>	<b>1</b>	4	<b>1</b>	<b>1</b>	5	6	
Multi-modal	F26	Best	505,971	517,909	509,950	502,985	522,092	506,965	501,990	538,322	503,980	
		Ave	517,476	560,970	537,666	512,536	548,476	524,498	509,864	546,953	513,426	
		Worst	532,353	633,320	574,621	526,864	608,605	546,763	514,924	558,471	527,937	
		Rank	5	10	7	3	9	6	2	8	4	
F27	Best	600,025	624,386	600,025	<b>600,000</b>	615,832	600,656	<b>600,000</b>	611,571	600,044	<b>600,000</b>	
		Ave	600,074	650,307	611,343	600,006	631,340	606,900	600,001	617,715	601,027	<b>600,000</b>
		Worst	600,149	667,079	639,107	600,156	654,192	625,713	600,001	624,853	607,000	<b>600,000</b>
		Rank	4	10	7	3	9	6	2	8	5	
F28	Best	715,714	805,633	736,669	714,309	722,773	720,757	715,907	756,171	715,519	711,920	
		Ave	726,902	814,637	761,643	722,469	771,793	748,504	721,959	773,760	731,182	716,659
		Worst	751,107	829,822	791,988	737,843	832,113	792,875	731,448	799,001	750,068	722,759
		Rank	4	10	7	3	8	6	2	9	5	
F29	Best	807,960	831,839	806,965	804,975	816,096	807,960	805,970	825,995	805,048	<b>802,985</b>	
		Ave	815,757	845,847	827,693	810,785	843,184	823,003	810,387	838,894	815,892	<b>808,039</b>
		Worst	825,870	886,560	853,667	821,889	887,651	847,758	816,914	855,237	838,836	<b>817,909</b>
		Rank	4	9	7	3	8	6	2	10	5	
F30	Best	<b>900,000</b>	1480,242	903,133	<b>900,000</b>	1017,191	907,182	<b>900,000</b>	936,214	900,017	<b>900,000</b>	
		Ave	900,008	1767,819	1084,271	900,102	1459,905	960,897	<b>900,000</b>	1002,447	910,685	<b>900,000</b>
		Worst	900,091	2215,333	1467,559	900,544	2193,418	1215,859	<b>900,000</b>	1105,444	949,156	<b>900,000</b>
		Rank	2	9	7	3	8	5	<b>1</b>	6	4	

**Table 5** (continued)

	Function	SMA	RFO	AVOA	EO	WOA	GTO	MPA	SCA	GWO	SWO
Hybrid	F31	Best	1408.041	1460.907	1441.596	1419.462	1503.978	1423.020	1400.001	1478.534	1445.514
	Ave	1462.045	3917.421	1755.072	1440.228	2052.400	1460.734	1404.079	1599.602	2971.692	1401.953
	Worst	1631.611	13,521.320	4065.479	1463.996	5361.819	1517.419	1421.249	1816.215	5769.769	1405.970
F32	Rank	5	10	7	4	8	3	1	6	9	1
	Best	1705.691	1741.150	1725.578	1702.010	1722.647	1719.161	1701.018	1748.169	1719.875	1700.058
	Ave	1759.494	1966.409	1761.930	1731.734	1791.076	1746.349	1715.586	1775.915	1756.583	1701.510
F33	Worst	1858.796	2254.981	1823.867	1783.388	1943.932	1789.102	1728.000	1801.979	1918.735	1703.619
	Rank	6	8	7	3	10	4	2	9	5	1
	Best	4594.171	3212.694	4549.959	1911.686	4215.803	1833.910	1800.083	40,425.390	3060.197	1800.002
F34	Ave	28,203.367	15,874.155	18,095.543	5459.247	21,249.755	2085.416	1800.972	128,450.239	26,579.781	1800.756
	Worst	53,527.584	47,351.759	39,474.991	17,231.483	38,466.026	3635.392	1806.773	413,594.948	55,123.601	1804.467
	Rank	9	5	6	4	7	3	2	10	8	1
F35	Best	1905.149	2017.269	1926.612	1905.415	2094.002	1902.015	1900.159	2003.469	1921.096	1900.019
	Ave	5417.756	5767.502	8509.347	1928.799	45,233.794	1956.375	1900.762	3741.379	6751.566	1900.087
	Worst	19,268.986	23,187.265	27,698.154	1999.866	424,612.729	2102.217	1901.439	12,799.591	15,398.964	1901.064
F36	Rank	6	7	9	3	10	4	2	5	8	1
	Best	2002.629	2056.896	2021.406	<b>2000.000</b>	2053.477	2021.307	2000.996	2065.956	2022.304	2000.000
	Ave	2023.800	2201.124	2107.599	2015.884	2161.801	2069.470	2012.021	2088.745	2090.548	2000.510
F37	Worst	2039.075	2429.361	2215.280	2141.626	2319.517	2190.345	2040.445	2131.522	2232.318	2004.292
	Rank	4	10	8	3	9	5	2	6	7	1

**Table 5** (continued)

	Function	SMA	RFO	AVOA	EO	WOA	GTO	MPA	SCA	GWO	SWO
Composition	F36	Best	2202.876	2201.432	<b>2200.000</b>	2214.369	<b>2200.000</b>	<b>2200.000</b>	2206.237	2200.511	<b>2200.000</b>
	Ave	2298.506	2328.951	2283.051	2301.575	2306.369	<b>2201.783</b>	2208.797	2259.955	2308.065	2214.042
	Worst	2340.272	2395.960	2377.102	2329.191	2384.552	<b>2203.682</b>	2310.239	2360.198	2345.624	2314.836
F37	Rank	6	10	5	7	8	<b>1</b>	2	4	9	3
	Best	2300.942	2305.197	2242.856	2300.000	2252.210	2240.844	<b>2200.000</b>	2312.362	2301.036	2218.076
	Ave	2368.387	2353.689	2306.698	2300.667	2509.032	2302.514	<b>2272.730</b>	2358.855	2363.755	2286.854
F38	Worst	3128.776	2457.060	2334.504	2301.546	4031.050	2321.333	<b>2301.085</b>	2403.773	3643.002	2301.311
	Rank	9	6	5	3	10	4	<b>1</b>	7	8	2
	Best	2611.676	2619.252	2613.376	2603.120	2620.787	2606.283	2604.813	2640.588	2605.280	<b>2603.081</b>
F39	Ave	2621.411	2710.705	2641.805	2612.265	2655.231	2622.138	2611.435	2657.542	2618.574	<b>2611.082</b>
	Worst	2637.064	2874.256	2663.923	2621.683	2726.690	2659.462	2620.130	2674.683	2636.734	<b>2620.894</b>
	Rank	5	10	7	3	8	6	2	9	4	<b>1</b>
F40	Best	2500.011	2500.007	2500.000	2724.740	2514.568	2500.000	2400.002	2542.674	2700.060	<b>2400.000</b>
	Ave	2746.008	2822.643	2747.150	2737.830	2775.345	2743.197	<b>2509.774</b>	2764.117	2744.499	2554.254
	Worst	2782.083	2979.588	2809.515	2755.165	2823.060	2779.259	<b>2743.285</b>	2793.021	2771.482	2751.880
	Rank	6	10	7	3	9	4	<b>1</b>	8	5	2
	Best	2900.005	2900.005	<b>2600.000</b>	<b>2600.000</b>	2824.825	<b>2600.000</b>	<b>2600.000</b>	3046.028	2832.150	<b>2600.000</b>
	Ave	3195.250	3645.284	3022.274	2881.017	3420.974	2934.122	<b>2816.001</b>	3082.538	3042.261	2888.000
	Worst	4154.345	4706.530	3305.150	3025.421	4276.486	3209.336	<b>2900.000</b>	3174.631	3950.833	<b>2900.000</b>
	Rank	8	10	5	2	9	4	<b>1</b>	7	6	3

**Table 5** (continued)

	Function	SMA	RFO	AVOA	EO	WOA	GTO	MPA	SCA	GWO	SWO
F41	Best	3159.724	3100.007	3100.000	3100.000	3104.570	3100.000	3100.000	3223.882	3164.958	<b>2800.000</b>
	Ave	3347.734	3325.453	3265.959	3283.751	3429.390	3256.088	3100.000	3269.399	3365.236	<b>3088.000</b>
	Worst	3731.813	3534.645	3411.822	3446.480	3749.371	3583.347	<b>3100.000</b>	3443.639	3506.386	<b>3100.000</b>
	Rank	9	8	5	7	10	3	2	6	4	1

*p*-values smaller than 5%

Bold values indicate the best outcomes

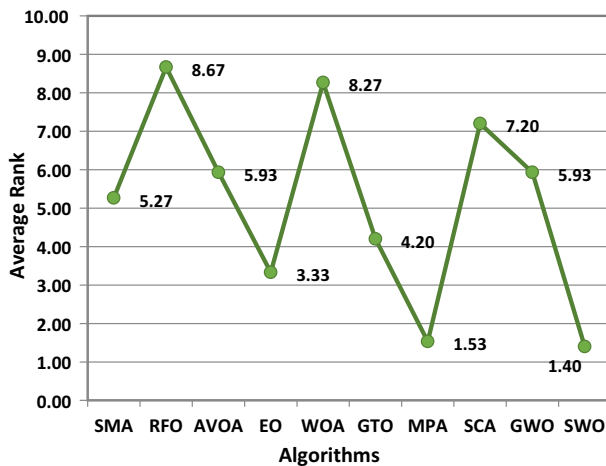
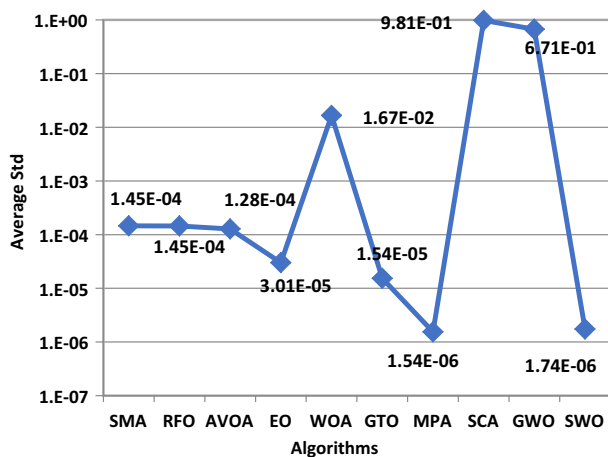


**Fig. 9** Average rank on all selected CEC-2017 functions

**Fig. 10** Average Std on all selected CEC-2017 functions



further investigate the performance of the newly introduced optimizer. The properties of those selected test functions are presented in Appendix A. The dimensions of all selected test functions of this suite are set to 10. Similar to the later sections, best, Ave, worst, and rank (based on Ave) of the fitness values obtained within 25 independent times are displayed in Table 5, in addition to the presented average rank and Std on all selected test functions through Figs. 9 and 10, respectively. This table shows that SWO is superior to all the rival methods for most selected test functions and competitive for the rest with high-performance optimizers, such as MPA, and GTO. Fig. 9 affirms that SWO comes in the first rank as the best optimizer, followed by MPA and RFO. In terms of the Std presented in Fig. 10, SWO is competitive with MPA. Finally, the p-values obtained by the Wilcoxon rank-sum statistical test between the SWO and each of the rival optimizers are presented in Table 6, which affirms the significant difference between the results of SWO and each of the optimizers because the p-values are less than 5% for most test functions with all rival optimizers.

**Table 6** p-Values of the Wilcoxon rank-sum test for F24-F41 (CEC-2017)

	Function	SMA	RFO	AVOA	EO	WOA	GTO	MPA	SCA	GWO
Wilcoxon	F24	<b>1.4140E - 09</b>	<b>1.4140E - 09</b>	<b>1.4140E - 09</b>	<b>1.4140E - 09</b>	<b>1.4140E - 09</b>	<b>1.4140E - 09</b>	<b>1.3340E - 08</b>	<b>1.4140E - 09</b>	<b>1.4140E - 09</b>
Rank-sum	F25	<b>1.0340E - 09</b>	<b>1.0340E - 09</b>	<b>1.0340E - 09</b>	<b>1.2760E - 08</b>	<b>1.0340E - 09</b>	<b>1.1360E - 07</b>	<b>1.0340E - 09</b>	<b>1.0340E - 09</b>	<b>1.0340E - 09</b>
test	F26	<b>5.5030E - 08</b>	<b>1.4020E - 09</b>	<b>2.5430E - 09</b>	<b>1.3150E - 03</b>	<b>1.4020E - 09</b>	<b>1.450E - 08</b>	<b>2.3110E - 03</b>	<b>1.4020E - 09</b>	<b>6.8280E - 04</b>
	F27	<b>1.8750E - 10</b>	<b>1.8750E - 10</b>	<b>1.8750E - 10</b>	<b>7.9170E - 10</b>	<b>1.8750E - 10</b>	<b>1.8750E - 10</b>	<b>1.8750E - 10</b>	<b>1.8750E - 10</b>	<b>1.8750E - 10</b>
	F28	<b>1.3090E - 07</b>	<b>1.4160E - 09</b>	<b>1.4160E - 09</b>	<b>2.2730E - 04</b>	<b>1.4160E - 09</b>	<b>2.2860E - 09</b>	<b>2.5490E - 05</b>	<b>1.4160E - 09</b>	<b>4.1020E - 07</b>
	F29	<b>2.1860E - 07</b>	<b>1.3930E - 09</b>	<b>1.0850E - 08</b>	<b>1.1900E - 02</b>	<b>1.5710E - 09</b>	<b>2.6570E - 08</b>	<b>2.9790E - 03</b>	<b>1.3930E - 09</b>	<b>3.4960E - 06</b>
	F30	<b>7.1880E - 10</b>	<b>7.1880E - 10</b>	<b>7.1880E - 10</b>	<b>7.6520E - 06</b>	<b>7.1880E - 10</b>				
	F31	<b>1.4070E - 09</b>	<b>1.4070E - 09</b>	<b>1.4070E - 09</b>	<b>1.4070E - 09</b>	<b>1.4070E - 09</b>	<b>1.4070E - 09</b>	<b>6.5910E - 03</b>	<b>1.4070E - 09</b>	<b>1.4070E - 09</b>
	F32	<b>1.4160E - 09</b>	<b>1.4160E - 09</b>	<b>1.4160E - 09</b>	<b>5.2120E - 09</b>	<b>1.4160E - 09</b>	<b>1.4160E - 09</b>	<b>1.9930E - 07</b>	<b>1.4160E - 09</b>	<b>1.4160E - 09</b>
	F33	<b>1.4160E - 09</b>	<b>1.4160E - 09</b>	<b>1.4160E - 09</b>	<b>1.4160E - 09</b>	<b>1.4160E - 09</b>	<b>1.4160E - 09</b>	<b>1.5110E - 01</b>	<b>1.4160E - 09</b>	<b>1.4160E - 09</b>
	F34	<b>1.4140E - 09</b>	<b>1.4140E - 09</b>	<b>1.4140E - 09</b>	<b>1.4140E - 09</b>	<b>1.4140E - 09</b>	<b>1.4140E - 09</b>	<b>4.9710E - 08</b>	<b>1.4140E - 09</b>	<b>1.4140E - 09</b>
	F35	<b>1.4470E - 09</b>	<b>1.2820E - 09</b>	<b>5.0140E - 07</b>	<b>1.2820E - 09</b>	<b>1.2820E - 09</b>	<b>3.7580E - 09</b>	<b>1.2820E - 09</b>	<b>1.2820E - 09</b>	<b>1.2820E - 09</b>
	F36	<b>2.0600E - 08</b>	<b>2.5770E - 08</b>	<b>1.0260E - 06</b>	<b>1.6400E - 06</b>	<b>2.8810E - 08</b>	<b>2.8400E - 02</b>	<b>4.9260E - 02</b>	<b>2.7520E - 07</b>	<b>2.5770E - 08</b>
	F37	<b>2.8980E - 09</b>	<b>1.4160E - 09</b>	<b>3.9960E - 08</b>	<b>1.4490E - 02</b>	<b>1.4650E - 08</b>	<b>1.6170E - 07</b>	<b>3.8260E - 01</b>	<b>1.4160E - 09</b>	<b>1.8000E - 09</b>
	F38	<b>7.5090E - 07</b>	<b>1.8000E - 09</b>	<b>5.2120E - 09</b>	<b>3.7210E - 01</b>	<b>1.5970E - 09</b>	<b>5.0070E - 05</b>	<b>8.3100E - 01</b>	<b>1.4160E - 09</b>	<b>6.6000E - 03</b>
	F39	<b>8.4930E - 09</b>	<b>9.5520E - 09</b>	<b>3.3110E - 08</b>	<b>6.83320E - 05</b>	<b>2.6240E - 09</b>	<b>4.1330E - 08</b>	<b>3.8650E - 03</b>	<b>4.7420E - 09</b>	<b>1.9090E - 06</b>
	F40	<b>1.0360E - 09</b>	<b>1.0360E - 09</b>	<b>2.6640E - 06</b>	<b>2.8770E - 02</b>	<b>1. - 08</b>	<b>2.3790E - 05</b>	<b>1.000E+00</b>	<b>1.0360E - 09</b>	<b>1.7590E - 08</b>
	F41	<b>8.3020E - 10</b>	<b>8.3020E - 10</b>	<b>7.6310E - 10</b>	<b>2.2750E - 09</b>	<b>8.2950E - 10</b>	<b>1.3640E - 09</b>	<b>8.3020E - 10</b>	<b>8.3020E - 10</b>	<b>8.3020E - 10</b>

*p*-values smaller than 5%

Bold values indicate the best outcomes

#### 4.4 Performance evaluation on the CEC-2014 test suite

Further validation is herein performed to check the performance of the introduced and other algorithms on the CEC-2014 test suite. This suite includes 30 test functions divided into unimodal, multimodal, hybrid, and composition to check the ability of an algorithm to explore, escape from local minima, and exploit. Accordingly, 12 test functions are selected with various types, including two unimodal, six multimodal, three hybrid, and two composition test functions, to observe the performance of SWO and competitors under various challenges. The properties of those selected test functions are presented in Appendix A, and their considered dimensions are 10. The best, Ave, and worst fitness values in addition to the rank metric are presented in Table 7, which illustrates that SWO is the best because it comes in the 1<sup>nd</sup> rank compared with all the rival algorithms on all observed functions, as affirmed by Fig. 11. Figure 12 reports the average Std of the fitness values on all selected CEC-2014. This figure shows that the outcomes obtained by SWO are significantly similar on each test function compared with the rival algorithms. Table 8 affirms that the outcomes obtained by SWO are significantly different compared with those of the competitors because the p-values of the Wilcoxon rank-sum statistical test are less than 0.05 for most test functions.

#### 4.5 Performance evaluation on the CEC-2020 test suite

Here, additional testing on the CEC-2020 test suite is carried out to verify the performance of the proposed SWO as well as the performance of competing methods. This suite, which consists of ten test functions and is broken down into unimodal, multimodal, hybrid, and compositional categories, can be used to evaluate an algorithm's capacity to explore, exploit, and avoid local minima. The attributes of this test suite are written out in Appendix A. The dimensions of this suite are set to 10 within the conducted experiments. Table 9 presents the best, average, and worst values obtained by analyzing the outcomes of 25 independent runs. This demonstrates that SWO has superior performance for most test functions in terms of the majority of the analysis indicators: Best, Ave, and worst, where it has superior values for 21 values out of 30 values, as shown in bold within Table 9.

The previous experiments show that SWO has strong exploration and exploitation operators in addition to having a high ability in balancing among those operators due to parameter TR, which has a significant effect on the performance of SWO. Increasing the value of this parameter promotes the exploitation operator, while decreasing it improves its exploration, and getting the optimal value will balance between two operators to be suitable for any issue. Finally, the experiments conducted affirm that SWO may be selected as an optimizer with high performance.

#### 4.6 Experimental convergence analysis of SWO

Figure 13 shows the performance of SWO in terms of diversity, convergence curve, average fitness history, and trajectory in the first dimension. This figure is divided into five columns: the first one depicts the topology of some test functions in two dimensions; the second one draws the average distance among agents through the optimization process to show diversity among them; the third one illustrates the convergence curve; the fourth one illustrates the averaged fitness history; and the last one illustrates the trajectory in the first dimension during the optimization process. In terms of the first metric known as diversity

**Table 7** Results of CEC-2014 test functions

	Function	SMA	RFO	AVOA	EO	WOA	GTO	MPA	SCA	GWO	SVO	
Unimodal	F42	Best	244.06435	206.01681	216.1236	2.09E+02	186.114.064	200.1812	2.00E+02	1.84E+08	5.08E+02	
		Ave	5764.4738	2324.1004	4940.653	9.09E+02	684.632.712	556.3063	2.00E+02	6.61E+08	2.42E+07	
		Worst	12,017.085	10,096.42	12,024.03	2.82E+03	1,474,838.87	2928.503	2.00E+02	1.57E+09	2.73E+08	
		Rank	7	5	6	4	8	3	2	10	9	
F43	Best	307.174	5424.738	631.713	303.278	17,141.513	300.000	300.000	2165.880	931.098	300.000	
		Ave	3008.011	18,774.079	1192.356	336.548	51,168.160	303.590	300.000	4695.023	5931.921	300.000
		Worst	12,087.402	54,693.753	2269.980	444.313	110,608.074	326.528	300.000	9724.119	14,480.094	300.000
		Rank	6	9	5	4	10	3	2	7	8	
Multi-modal	F44	Best	400.144	400.017	400.000	404.335	400.785	400.000	400.000	418.712	400.536	
		Ave	426.899	430.038	426.782	428.695	436.015	418.811	406.952	459.090	432.598	
		Worst	435.022	495.914	469.533	434.780	487.646	434.780	434.780	540.471	515.707	
		Rank	5	7	4	6	9	3	2	10	8	
F45	Best	600.657	607.431	602.779	600.000	605.426	601.984	600.004	604.042	600.789	600.000	
		Ave	604.662	610.247	605.578	600.770	607.886	605.255	600.224	606.817	602.290	
		Worst	607.504	611.819	608.906	604.830	610.559	608.914	601.062	609.220	604.076	
		Rank	5	10	7	3	9	6	2	8	4	
F46	Best	700.083	700.605	700.091	700.007	700.498	700.096	700.012	704.724	700.107	700.007	
		Ave	700.230	704.096	700.370	700.042	701.269	700.310	700.044	710.755	700.987	700.029
		Worst	700.571	714.746	700.935	700.153	703.039	700.993	700.113	716.355	702.392	700.074
		Rank	4	9	6	2	8	5	3	10	7	

**Table 7** (continued)

	Function	SMA	RFO	AVOA	EO	WOA	GTO	MPA	SCA	GWO	SWO
F47	Best	800.000	816.914	802.985	800.995	815.084	806.965	800.995	827.288	803.987	<b>800.000</b>
	Ave	801.553	854.093	815.243	804.656	841.979	823.494	803.542	838.094	808.448	<b>800.000</b>
	Worst	803.980	883.763	826.864	812.934	876.630	845.768	806.965	854.058	820.237	<b>800.000</b>
Rank	2	10	6	4	9	7	3	8	5	1	<b>1</b>
	Best	904.976	926.864	911.939	905.970	918.138	906.965	906.965	931.469	905.970	<b>900.995</b>
	Ave	918.598	950.424	928.894	912.138	950.246	928.336	911.223	942.380	915.224	<b>908.198</b>
Rank	5	10	7	3	8	6	2	9	4	1	<b>15.919</b>
	Best	1003.662	1692.614	1049.081	1000.375	1020.267	1042.501	1003.665	1592.341	1086.816	<b>1000.125</b>
	Ave	1155.228	2289.300	1195.132	1116.642	1563.303	1466.145	1078.942	1955.487	1331.739	<b>1001.098</b>
Rank	4	10	5	3	8	7	2	9	6	1	<b>1011.892</b>
	Best	1900.721	1904.040	1901.694	1900.155	1903.078	1900.294	1900.134	1903.690	1901.294	<b>1900.037</b>
	Ave	1901.781	1911.046	1903.211	1900.707	1906.044	1902.064	1900.971	1905.094	1902.639	<b>1900.286</b>
Rank	5	10	7	2	9	4	3	8	6	1	<b>1901.023</b>
	Best	2234.506	2592.151	2467.428	2105.583	5057.319	2100.666	2100.380	3817.802	2418.472	<b>2100.031</b>
	Ave	4281.055	9094.341	12,273.102	2242.083	84,916.947	2445.785	2101.924	11,783.533	9122.050	<b>2103.956</b>
Rank	4	11,523.864	25,720.494	29,685.732	2504.409	557,790.038	2758.418	2117.449	34,928.768	16,029.082	<b>2117.198</b>
	Best	2227.771	2220.880	2200.236	2228.239	2200.511	2200.129	2242.976	2221.561	2221.561	<b>2200.001</b>
	Ave	2230.892	2543.871	2258.302	2239.978	2276.274	2242.713	2210.941	2262.652	2278.695	<b>2200.280</b>
Rank	3	6	7	4	9	5	2	8	10	1	<b>2200.567</b>

**Table 7** (continued)

	Function	SMA	RFO	AVOA	EO	WOA	GTO	MPA	SCA	GWO	SWO
Composition	F53	Best	2500.000	2500.000	2500.000	2629.457	2500.000	2500.000	<b>2300.000</b>	2635.109	2629.474
		Ave	2500.000	2500.000	2500.000	2629.457	2627.153	2500.000	2597.923	2642.942	2633.580
		Worst	<b>2500.000</b>	<b>2500.000</b>	<b>2500.000</b>	2629.457	2637.342	<b>2500.000</b>	2629.457	2653.271	2639.520
		Rank	3	3	3	6	5	2	4	8	7
F54	Best	2703.086	2900.000	2900.000	<b>2701.541</b>	2708.689	2703.489	2702.047	2708.299	2703.696	2702.275
		Ave	2892.123	2900.000	2900.000	2991.977	3112.272	2868.913	2828.994	3011.577	3021.034
		Worst	2900.000	2900.000	2900.000	3100.363	3254.319	2900.000	3100.133	3107.664	3102.122
		Rank	4	5	5	6	9	3	2	7	8

*p*-values smaller than 5%

Bold values indicate the best outcomes

**Fig. 11** Average rank on all selected CEC-2014 functions

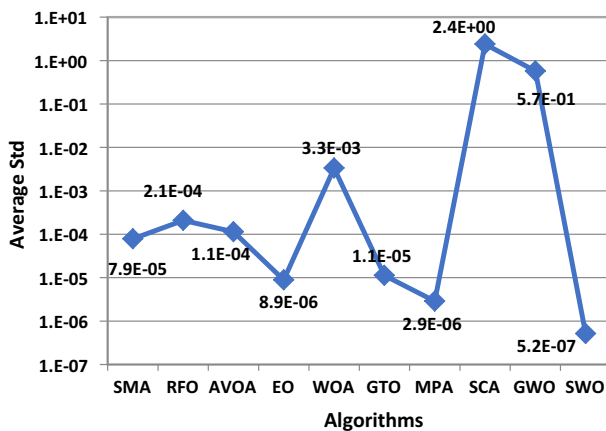
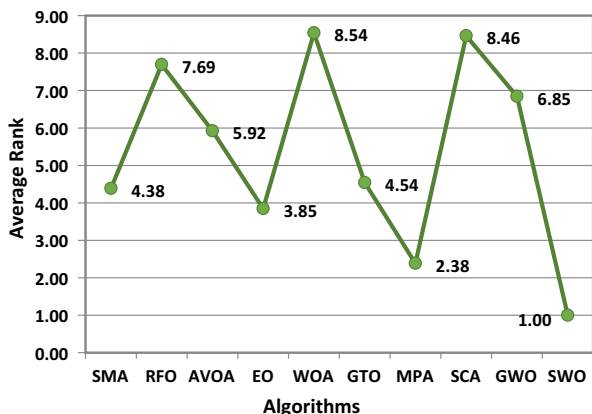


**Fig. 12** Average Std on all selected CEC-2017 functions

among agents, the second column in Fig. 13 shows the averaged distance among agents through each iteration to show shifting from exploration into exploitation. This column shows a decreasing trend in all figures and the gradual shift of SWO from exploration to exploitation. Moreover, this figure elaborates that the diversity is again increased during the optimization process, exhibiting the ability of the introduced method to improve its diversity during the process for escaping from the local minima to reach better outcomes.

The second column in this figure contains the convergence curve of SWO. This column shows no change in the convergence curve through a range of iterations due to the application of the exploration phase to the global search domain to find better results; hence, this curve takes the form of a step-like pattern, especially in multimodal, hybrid, and composition test functions. The convergence curve reports the behavior of the best agent for finding a better solution without giving any illustration to the performance of the whole population. Therefore, another metric called average fitness history is utilized to compute the average of the fitness values for all solutions in the iteration process. The average fitness history presented in the third column in Fig. 13 demonstrates the variation tendency of the fitness values obtained by the solutions during the optimization process. In the last

**Table 8** p-Values of the Wilcoxon rank-sum test for F42-F54 (CEC-2014)

	Function	SMA	RFO	AVOA	EO	WOA	GTO	MPA	SCA	GWO
Wilcoxon	F42	<b>1.1200E - 09</b>								
Rank-sum	F43	<b>1.4090E - 09</b>								
test	F44	<b>4.5270E - 07</b>	<b>2.2050E - 07</b>	<b>6.7320E - 06</b>	<b>1.7080E - 08</b>	<b>5.0100E - 07</b>	<b>2.0600E - 04</b>	<b>8.7660E - 01</b>	<b>2.2760E - 09</b>	<b>1.4500E - 07</b>
	F45	<b>1.8000E - 09</b>	<b>1.4160E - 09</b>	<b>1.4160E - 09</b>	<b>4.9020E - 03</b>	<b>1.4160E - 09</b>	<b>1.4160E - 09</b>	<b>5.8660E - 03</b>	<b>1.4160E - 09</b>	<b>7.3800E - 09</b>
	F46	<b>1.4140E - 09</b>	<b>1.4140E - 09</b>	<b>1.4140E - 09</b>	<b>2.6040E - 01</b>	<b>1.4140E - 09</b>	<b>1.4140E - 09</b>	<b>1.1650E - 02</b>	<b>1.4140E - 09</b>	<b>1.4140E - 09</b>
	F47	<b>3.8500E - 10</b>	<b>3.8500E - 10</b>	<b>3.8460E - 10</b>	<b>3.8220E - 10</b>	<b>3.8500E - 10</b>				
	F48	<b>2.6220E - 06</b>	<b>1.3830E - 09</b>	<b>2.8310E - 09</b>	<b>7.5290E - 04</b>	<b>1.3830E - 09</b>	<b>1.1420E - 08</b>	<b>5.8940E - 4</b>	<b>1.3830E - 09</b>	<b>2.7450E - 05</b>
	F49	<b>2.0250E - 09</b>	<b>1.4130E - 09</b>	<b>1.4120E - 09</b>	<b>6.9430E - 09</b>	<b>1.4130E - 09</b>	<b>1.4130E - 09</b>	<b>2.0250E - 09</b>	<b>1.4130E - 09</b>	<b>1.4130E - 09</b>
	F50	<b>2.2890E - 09</b>	<b>1.4160E - 09</b>	<b>1.4160E - 09</b>	<b>6.9620E - 05</b>	<b>1.4160E - 09</b>	<b>7.3800E - 09</b>	<b>1.6170E - 07</b>	<b>1.4160E - 09</b>	<b>1.4160E - 09</b>
	F51	<b>1.4160E - 09</b>	<b>1.4160E - 09</b>	<b>1.4160E - 09</b>	<b>2.5740E - 9</b>	<b>1.4160E - 09</b>	<b>1.4650E - 08</b>	<b>9.5190E - 02</b>	<b>1.4160E - 09</b>	<b>1.4160E - 09</b>
	F52	<b>7.3800E - 09</b>	<b>1.4160E - 09</b>	<b>1.4160E - 09</b>	<b>2.0540E - 08</b>	<b>1.4160E - 09</b>	<b>1.8000E - 09</b>	<b>1.1600E - 05</b>	<b>1.4160E - 09</b>	<b>1.4160E - 09</b>
	F53	<b>3.3710E - 01</b>	<b>3.3710E - 01</b>	<b>3.3710E - 01</b>	<b>7.0330E - 11</b>	<b>1.3760E - 10</b>	<b>3.3710E - 01</b>	<b>6.7240E - 08</b>	<b>1.3760E - 10</b>	<b>1.3760E - 10</b>
	F54	<b>8.7610E - 10</b>	<b>9.7280E - 11</b>	<b>9.7280E - 11</b>	<b>1.9670E - 05</b>	<b>1.4160E - 09</b>	<b>1.0010E - 09</b>	<b>1.8060E - 01</b>	<b>1.4160E - 09</b>	<b>3.2610E - 09</b>

p-values smaller than 5%

Bold values indicate the best outcomes

**Table 9** Results of CEC-2020 test functions

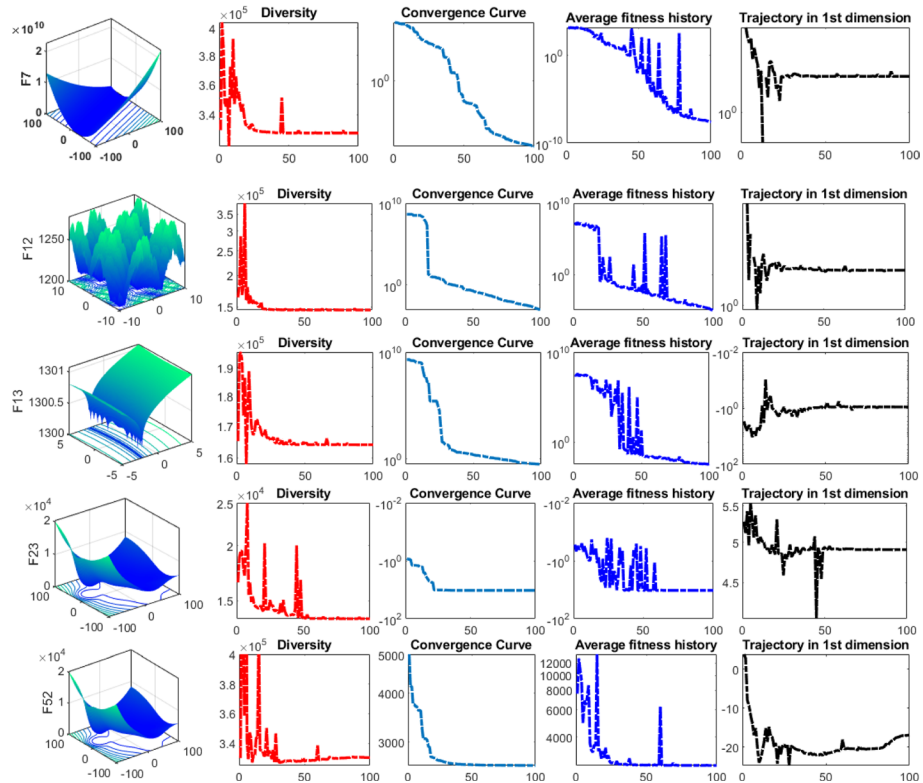
Function	SMA	RFO	AVOA	EO	WOA	GTO	MPA	SCA	GWO	SWO
F55	Best	107.5038	1.256E+08	1.004E+02	2.952E+10	1.173E+05	100.3943	100.0000	3.932E+08	1.541E+03
	Ave	7623.884	1.250E+10	3.146E+03	4.682E+10	2.094E+06	1762.2036	100.0000	7.573E+08	5.116E+07
	Worst	12.734.0640	1.820E+10	1.276E+04	6.191E+10	1.0706E+07	6620.5661	100.0001	1.506E+09	3.830E+08
F56	Best	1245.3286	1802.2207	1466.0822	3245.6618	1336.3556	1235.2633	1115.3669	1709.5445	1107.4439
	Ave	1612.6132	2484.1297	1968.2818	3292.4896	2076.5144	1944.5639	1353.6824	2265.2643	1537.8511
	Worst	1989.9464	3124.6609	2494.9991	3428.1026	2810.6589	2549.1936	1710.8750	2621.5549	2072.0480
F57	Best	712.5953	811.2897	723.1690	2500.3613	743.9142	729.132	716.803	763.5178	713.7184
	Ave	724.2026	815.4422	761.2900	2671.2296	780.8330	752.2226	723.3470	775.6098	733.0892
	Worst	734.5032	826.5141	786.3277	280.9541	816.9402	785.265	730.903	789.4484	783.7408
F58	Best	1900.0000	1900.0000	1900.0000	4.006.907.1122	1900.0000	1900.0000	1900.0000	1900.0000	1900.0000
	Ave	1900.0000	1900.0000	1900.0000	4.006.907.1122	1900.0094	1900.0000	1900.0000	1900.0000	1900.0000
	Worst	1900.0000	1900.0000	1900.0000	4.006.907.1122	1900.2816	1900.0000	1902.0481	1901.5434	1900.6017
F59	Best	1819.5945	1.85E+04	2331.8678	4.78E+08	3.56E+03	1867.1687	1702.1985	6090.4031	3448.9023
	Ave	8936.9912	8.56E+05	7718.4772	4.78E+08	1.19E+05	2298.3940	1717.6774	34.040.2350	28.673.8938
	Worst	18.970.7803	3.93E+06	23.108.0958	4.78E+08	6.95E+05	2686.6521	1750.1786	313.748.1801	347.488.4669
F60	Best	1601.5573	1776.0661	1601.6767	2516.8559	1629.4684	1601.8014	1600.4096	1622.6320	1601.7266
	Ave	1716.9061	2259.1275	1761.4453	2676.0727	1842.9864	1733.6781	1601.5984	1766.8708	1756.1550
	Worst	1945.0146	2817.4889	1977.9791	2832.2393	2101.6511	1970.3711	1612.4422	1942.9789	1943.8380
F61	Best	2137.9566	3.95E+03	2209.8743	3.541.094.3754	4347.9936	2101.1550	2100.4348	3825.6938	2343.6754
	Ave	3731.1318	2.82E+06	9964.3588	3.541.288.5939	47.610.4269	2395.8324	2101.0760	9976.8331	14.921.4756
	Worst	14.760.7070	1.31E+07	27.784.1208	3.542.025.6782	422.173.1436	2891.3274	2102.7260	28.709.1509	202.281.9232
F62	Best	2228.4437	2531.1994	2228.5788	4655.5101	2304.2059	2302.0872	2200.0000	2339.7532	2301.0065
	Ave	2425.2558	3607.8696	2305.1423	4717.3119	2369.0414	2307.3006	2276.4632	2376.1533	2363.9942
	Worst	3364.4754	4551.0382	2319.1817	4887.2668	3924.3715	2328.6001	2301.8406	2479.0383	3152.3304
F63	Best	2740.5883	2712.5198	2500.0000	2928.4369	2509.0376	2500.0000	2500.0000	2540.1823	2725.4675
	Ave	2755.6396	2927.5182	2722.9248	2949.9112	2760.7517	2711.6977	2516.8299	2768.9683	2749.9163
	Worst	2775.2683	3097.5251	2813.4879	2976.0120	2837.2971	2790.9349	2601.9909	2806.4450	2801.4819

**Table 9** (continued)

Function	SMA	RFO	AVOA	EO	WOA	GTO	MPA	SCA	GWO	SWO
F64	Best	2898.0864	3234.0496	2897.7429	6385.1528	2784.0709	2897.7429	<b>2897.7429</b>	2921.9408	2898.2812
	Ave	2931.5098	3634.2218	2940.2067	9386.3879	2938.9053	2925.3763	2899.4673	2952.9393	2938.7951
	Worst	2971.0872	3928.0002	3024.3333	10,653.8810	2999.2284	2949.5108	<b>2943.5124</b>	2976.2229	3024.4618

*p*-values smaller than 5%

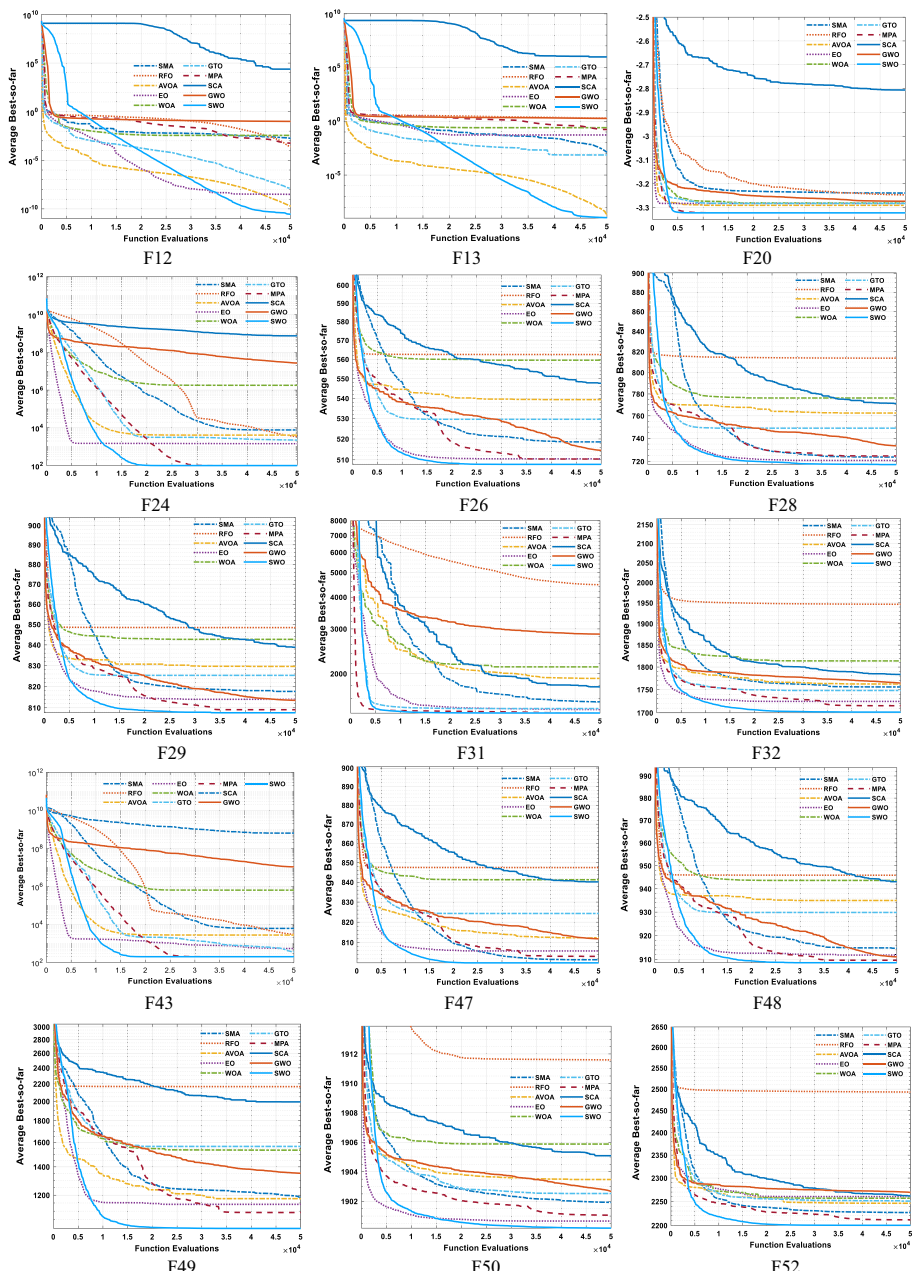
Bold values indicate the best outcomes



**Fig. 13** Diversity, convergence curve, average fitness history, and trajectory

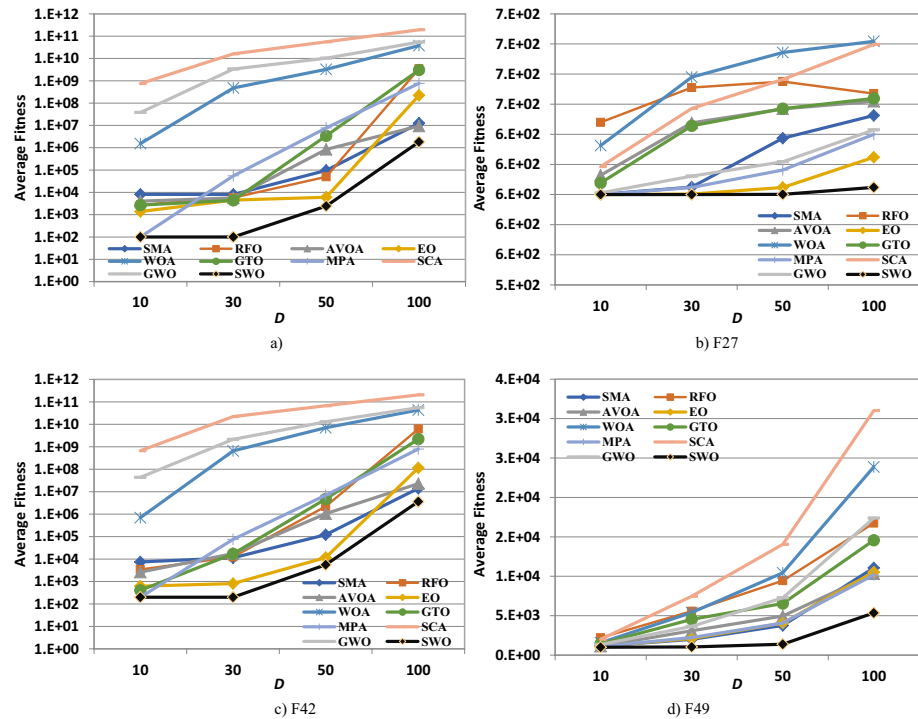
half of the optimization process, this variation is minimized, and the average fitness value in the right direction of the near-optimal solution is decreased. The last metric displayed in the last column in Fig. 13 is the trajectory in the first dimension. The last column shows that changes in this dimension have high frequency and magnitude at the start of the optimization process and gradually fade out with increasing iteration. This trend affirms that SWO has strong explorative behavior in initial iterations, which subsequently gives way to exploitation operator in order to steer convergence toward the nearly optimal solution.

Figure 14 shows the convergence curve of SWO and rival methods on some test functions to further show their characteristics. The results presented in this figure indicate a couple of outstanding patterns that mark the proposed algorithm for optimizing the optimization problems. Those patterns are mainly due to the hunting and nesting behaviors and mating behavior. In the hunting and nesting behavior, population updating is based on two phases. The first phase will require the whole population at the start of the optimization process to explore the search space to escape the local minima trap for reaching the promising region that includes the near-optimal solution. The first phase also involves the updating strategy of mating behavior, wherein the algorithm will explore the regions around the current solution; however, this behavior will extend even the end of the optimization process to help in escaping from the local minima through the whole optimization process. Figure 14 elaborates a slow convergence speed in the right direction of the near-optimal



**Fig. 14** Averaged convergence curve for each algorithm on various mathematical test functions

solution within the first phase because the algorithm focuses its searching for the promising region as much as possible without drifting to the best-so-far solution, which might be a trap. The second phase will gradually draw a portion of the population to focus on the promising region, which will result in a significant increase in convergence speed and more



**Fig. 15** Scalability analysis of SWO

improvements, as shown in Fig. 14. Thus, SWO could outperform all the rival methods in terms of convergence speed for all the test functions observed in Fig. 14 due to its ability to avoid stuck into local minima.

#### 4.7 Scalability analysis of SWO

This section validates the performance of SWO for high-dimensional test functions compared with the rival optimizers. Four test functions with different types, namely, F24, F27, F42, and F49, have been selected for scalability analysis. All algorithms have been investigated under 10, 30, 50, and 100 dimensions for those four test functions to observe their scalability when increasing the size of the dimensions. Figure 13 shows the average fitness values obtained by each algorithm on those test functions over 10, 30, 50, and 100 dimensions. Figure 15a shows the superiority of SWO over all dimensions compared with all rival algorithms except for  $D=10$ , which is also solved by MPA, using F24 as the starting point. Passing to F27, Figure 15b affirms the superiority of the suggested algorithm in tackling high-dimensional test functions, where it could overcome most algorithms and compete with the others over all the observed dimensions. F42 and F49 solved in Fig. 15c, d by the algorithms further affirm that SWO has strong performance when increasing the size of dimensions. This section elaborates that SWO has superior performance compared with all the rival algorithms when dealing with high-dimensional problems.

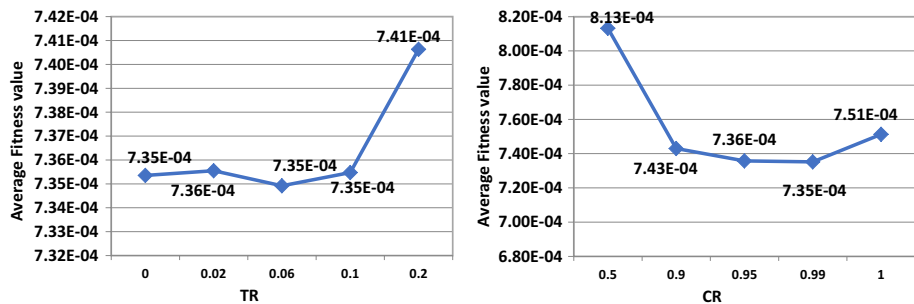


**Fig. 16** Tuning of parameters **TR** and **CR** over DDM

## 5 Real-world optimization problems

This section investigates the performance of SWO in two different types of real-world optimization problems. The first type is constrained engineering design problems, such as WBD and pressure vessel design. Meanwhile, the second type is estimating the unknown parameters of the photovoltaic models, including the SDM, double-diode model (DDM), and three diode model (TDM). A simple penalty method is integrated for constrained engineering design problems to convert the constrained problems into unconstrained ones. All algorithms are executed under the same parameters described before. However, the introduced algorithm has a number of parameters that need to be tackled for to improve its performance during solving any optimization problem. Hence, the parameters of the proposed will be adjusted in the next subsection. Algorithms with more parameters might increase their applicability for various optimization problems due to diversifying searching manners, which need to be accurately adjusted by the controlling parameters.

### 5.1 Parameter tuning of SWO for real-world problems

As previously mentioned, the SWO algorithm has three effective parameters: TR, CR, and  $N_{min}$ , which have to be accurately estimated to increase its performance when dealing with different optimization problems. In this part, some real-world optimization problems with different natures will be solved by SWO to investigate its performance. Accordingly, these parameters have to be first estimated to adapt the SWO's performance to this type of problem. The first experiment investigates the performance of SWO under various values for TR, such as 0, 0.02, 0.06, 0.1, and 0.2, to obtain the best one among them. Figure 16a reports the results of this experiment. This figure demonstrates the superior performance under a value of 0.06 for TR.

The second experiment is herein conducted to find the optimal value for the parameter CR. In this experiment, five values (0.5, 0.9, 0.95, 0.99, and 1.0) for this parameter are observed to see the influence of each one on the proposed algorithm: SWO. Figure 16b presents the findings of this experiment, which affirms that SWO under a value of 0.99 for CR performs better. The last experiment detects the best value for  $N_{min}$  among six values: 10, 15, 25, 35, 45, and 50 with constant value of  $N$  to 50. The outcomes of this experiment are depicted in Fig. 17 over DDM and TDM. The best value for this parameter for those two models is 25.

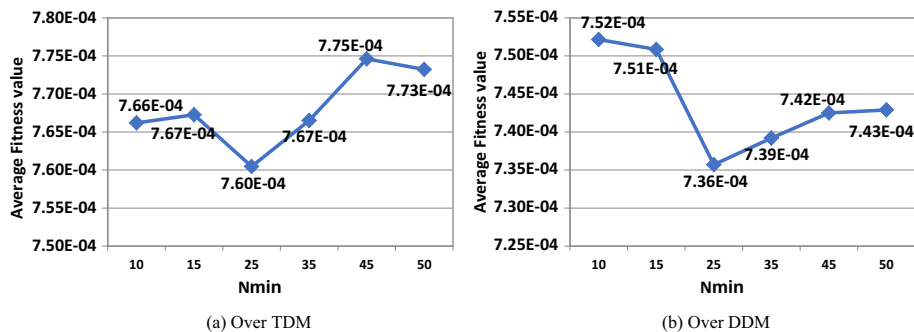


**Fig. 17** Tuning of parameters  $N_{\min}$  over DDM and TDM

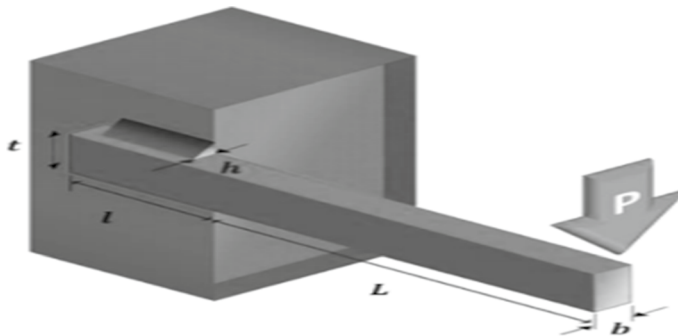


**Fig. 18** Structure of WBD (Faramarzi et al. 2020b)

## 5.2 Engineering design problems

The first investigated constrained problem in engineering is a welded beam design (WBD), which is depicted in Fig. 18. The objective of this problem is to find the near-optimal solution for four parameters ( $h$ ,  $l$ ,  $t$ , and  $b$ ) that minimize the total fabrication cost of a welded beam. This solution has to be subject to seven constraints, namely, shear stress, bending stress, tip detection, weld coverage, buckling load, weld thickness, and cost. The formulation of this problem is listed below:

- The four parameters are represented as follows:

$$X = [x_1 x_2 x_3 x_4] = [h l t b]$$

- The objective function is formulated as:

$$f(X) = 1.10471x_1^2x_2 + 0.04811x_3x_4(14.0 + x_2)$$

- The mathematical formulations of constraints are as follows:

$$g_1(X) = \tau(X) - \tau_{max} \leq 0$$

$$g_2(X) = \sigma(X) - \sigma_{max} \leq 0$$

$$g_3(X) = \delta(X) - \delta_{max} \leq 0$$

$$g_4(X) = x_1 - x_4 \leq 0$$

$$g_5(X) = P - P_c(X) \leq 0$$

$$g_6(X) = 0.125 - x_1 \leq 0$$

$$g_7(X) = 1.10471x_1^2 + 0.04811x_3x_4(14.0 + x_2) - 5.0 \leq 0$$

where

$$\tau(X) = \sqrt{(\tau')^2 + \frac{2\tau'\tau''x_2}{2R} + (\tau'')^2}$$

$$\tau' = \frac{P}{\sqrt{2}x_1x_2}, \tau'' = \frac{MR}{J}, M = P\left(L + \frac{x_2}{2}\right)$$

$$R = \sqrt{\frac{x_2^2}{4} + \left(\frac{x_1 + x_3}{2}\right)^2}$$

$$J = 2 \left\{ \sqrt{2}x_1x_2 \left[ \frac{x_2^2}{12} + \left(\frac{x_1 + x_3}{2}\right)^2 \right] \right\}$$

$$\sigma(X) = \frac{6PL}{x_4x_3^2}, \delta(X) = \frac{6PL^3}{Ex_3^2x_4}$$

$$P_c(X) = \frac{4.0134E\sqrt{\frac{x_3^2x_4^6}{36}}}{L^2} \left( 1 - \frac{x_3}{2L} \sqrt{\frac{E}{4G}} \right)$$

$$P = 6000, L = 14, E = 30 \times 10^6, G = 12 \times 10^6$$

$$\tau_{max} = 13600, \sigma_{max} = 30000, \delta_{max} = 0.25$$

Table 10 shows the outcomes of SWO and rival methods for this problem. This table affirms that the introduced algorithm could reach the optimal value. Figure 20a depicts the convergence speed of each algorithm for the WBD problem. This figure shows the high ability of SWO to minimize the objective function in a small number of function evaluations (up to 5000). Thus, SWO outperforms the other algorithms in terms of

**Table 10** Comparison among algorithms over the WBD problem

Algorithms	$x_1$	$x_2$	$x_3$	$x_4$	Best	Ave	Worst	Std	Rank
SMA	0.205712	3.470773	9.036859	0.205728	1.72489538	1.72599910	1.74098916	2.90E - 03	4
RFO	0.200028	3.594915	9.045035	0.205721	1.73401168	1.99120454	2.42401619	1.91E - 01	9
AVOA	0.205588	3.473533	9.036618	0.205730	1.72504501	1.73964239	1.79645483	1.76E - 02	6
EO	0.205720	3.470704	9.036624	0.205730	1.72486585	1.72510970	1.72951890	8.84E - 04	3
WOA	0.197415	3.574336	9.514330	0.203463	1.79061977	2.31415795	4.64365674	6.98E - 01	10
GTO	0.205720	3.470704	9.036624	0.205730	1.72486585	1.78354948	2.60274689	2.21E - 01	7
MPA	0.205720	3.470704	9.036624	0.205730	1.72486585	1.72486587	1.72486592	1.60E - 08	2
SCA	0.188440	3.867919	9.080050	0.207676	1.77273347	1.85854497	1.93269845	3.64E - 02	8
GWO	0.205670	3.472321	9.036206	0.205760	1.72517005	1.72602592	1.72738191	6.18E - 04	5
SWO	<b>0.205720</b>	<b>3.470704</b>	<b>9.036624</b>	<b>0.205730</b>	<b>1.72486585</b>	<b>1.72486585</b>	<b>1.72486585</b>	<b>2.26E - 16</b>	<b>1</b>

*p*-values smaller than 5%

Bold values indicate the best outcomes

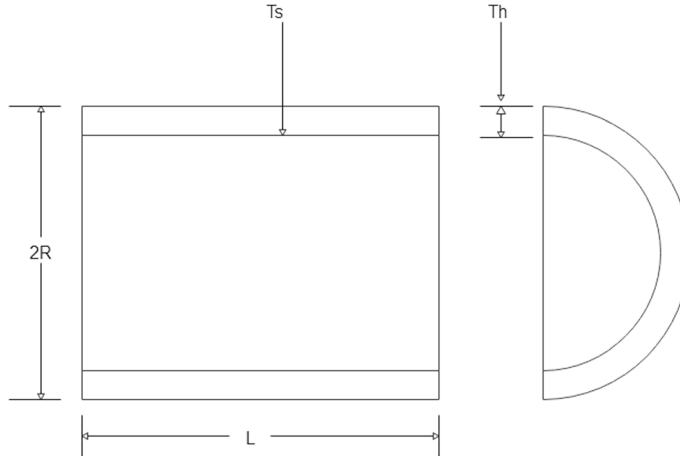


**Fig. 19** Structure of pressure vessel

finding the near-optimal values of design variables that minimize the total fabrication cost.

The second problem is the pressure vessel design, which has also four parameters that have to be accurately estimated to minimize the total production cost and are subject to the pressure requirements. These parameters are inner radius ( $R$ ), thickness of the shell ( $Ts$ ), thickness of the head ( $Th$ ), and cylindrical portion length ( $L$ ). The structure of the pressure vessel is illustrated in Fig. 19. The mathematical model of this problem is designed below (Li et al. 2020):

- The four parameters are represented as follows:

$$X = [x_1 x_2 x_3 x_4] = [Ts Th RL]$$

**Table 11** Comparison among algorithms over the pressure vessel design problem

Algorithms	$x_1$	$x_2$	$x_3$	$x_4$	Best	Ave	Worst	Std	Rank
SMA	0.778449	0.384793	40.333647	199.804812	5885.89721	6365.53066	7319.11013	5.65E–02	5
RFO	0.782594	0.386842	40.547943	196.911481	5894.51091	49.467.64615	260.843.5333	6.33E–02	10
AVOA	0.780207	0.385662	40.424727	198.541966	5888.91070	6514.65833	7319.11358	2.68E–02	6
EO	0.790387	0.395580	40.952184	191.377764	5921.20339	6326.47577	6701.03941	5.88E–04	3
WOA	0.854003	0.433458	44.245548	151.730888	6067.81295	8052.71837	12.458.7141	2.56E–02	9
GTO	0.778179	0.384659	40.319627	199.999891	5885.43443	6484.45765	7319.11379	2.15E–02	7
MPA	0.778179	0.384659	40.319619	200.000000	5885.43418	5885.43422	5885.43431	2.84E–03	2
SCA	0.785562	0.406981	40.658585	200.000000	6060.72295	6742.29490	8263.76113	3.60E–03	8
GWO	0.778262	0.385194	40.319869	200.000000	5887.62287	6002.86301	7245.07047	1.88E–02	4
SWO	<b>0.778179</b>	<b>0.384659</b>	<b>40.319619</b>	<b>200.000000</b>	<b>5885.43417</b>	<b>5885.43417</b>	<b>5885.43417</b>	<b>1.11E–05</b>	<b>1</b>

- The objective function is formulated as follows:

$$f(X) = 0.6224x_1x_3x_4 + 1.7781x_3x_1^2 + 3.1661x_4x_1^2 + 19.84x_3x_1^2$$

- The mathematical formulations of the constraints are as follows:

$$g_1(X) = -x_1 + 0.0193x_3 \leq 0$$

$$g_2(X) = -x_3 + 0.00954x_3 \leq 0$$

$$g_3(X) = -\pi x_4x_3^2 - \frac{4}{3}x_3^3 + 1296000 \leq 0$$

$$g_4(X) = x_4 - 240 \leq 0$$

In this section, SWO is also validated on the pressure vessel design problem and compared with nine rival methods, such as SMA, RFO, AVOA, EO, WOA, GTO, MPA, SCA, and GWO. The results of executing each algorithm 30 times for each algorithm is analyzed in terms of the best, Ave, Worst, Std, and Rank (based on Ave) in addition to the best-obtained parameters presented in Table 11, that affirms the superiority of the introduced method for all performance metrics. Figure 20b shows that SWO is the first for reaching the lowest fitness value in terms of the convergence speed.

### 5.3 Parameter estimation problem of the PV models

In this section, SWO is evaluated using the SDM, DDM, and triple-diode model (TDM) based on the R.T.C France cell. The current–voltage data is measured on a 57 mm diameter commercial silicon R.T.C. France solar cell under  $1000 \text{ W/m}^2$  at  $33^\circ\text{C}$  (Easwarakhanthan et al. 1986). These models involve the parameter that is not introduced in the manufacturing sheet and needs to be accurately optimized to accurately and effectively implement each model. The upper and lower bounds of these unknown parameters are reported in Table 12 as widely employed in the published papers (Gong and Cai 2013; Yu et al. 2017; Yu et al. 2018; Chen et al. 2018; Li et al. 2019). The objective of this problem is to find the values of the unknown parameters that minimize the root mean squared error (RMSE) between the measured and

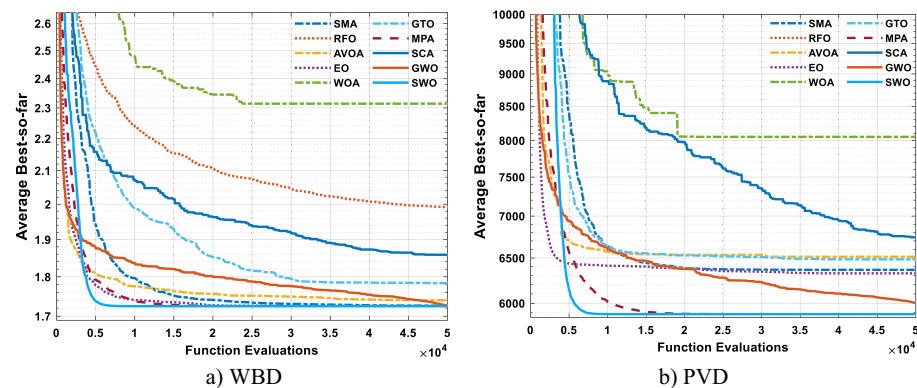


**Fig. 20** Averaged convergence curve for each algorithm on WBD and PVD

**Table 12** Lower and upper bound of the unknown parameters

Parameter	R.T.C France cell	
	$L_b$	$U_b$
$I_{ph}(A)$	0	1
$I_{sd}, I_{sd1}, I_{sd2} (A)$	0	$1 \times 10^{-6}$
$R_s(\Omega)$	0	0.5
$R_{sh}(\Omega)$	0	100
$n, n_1, n_2$	1	2

estimated current. RMSE is the objective function of this problem and is mathematically formulated as follows:

$$RMSE = f(X_i) = \sqrt{\frac{1}{M} * \sum_{k=1}^M (I_m - I_e(V_e, X_i))^2}$$

where  $I_e$  indicates the estimated current and discussed in detail in the next section on the account of the PV model,  $I_m$  indicates the measured current,  $M$  indicates the number of measured data,  $X_i$  is the obtained parameters by the  $i^{th}$  solution, and  $I_e$  is computed based on the obtained parameters and Newton–Raphson according to the following (Nunes et al. 2018).

### 5.3.1 SDM

In SDM, the SDM output symbolized as  $I$  is computed utilizing the following equation:

$$I = I_{ph} - I_D - I_{sh}$$

where  $I_{ph}$  indicates the photo-generated current (Tan et al. 2004), and  $I_D$  represents the diode current and calculated according to the following formula:

**Table 13** Results of SDM compared with the rival methods

Algorithms	Best-obtained parameters					RMSE				
	$I_{ph}$ (A)	$I_{sd}$ (μA)	$R_s$ (Ω)	$R_{sh}$ (Ω)	$n$	<i>Best</i>	<i>Worst</i>	<i>Ave</i>	<i>Std</i>	<i>Rank</i>
SMA	0.7603	1.2261E - 07	4.0638E - 02	46.0875	1.3893	1.6961E - 03	8.7570E - 03	7.2983E - 03	1.4925E - 03	10
RFO	0.7685	1.0000E - 09	5.4224E - 02	13.0683	1.0634	8.0640E - 03	1.0211E - 01	5.8314E - 02	3.4276E - 02	9
AVOA	0.7611	6.7490E - 07	3.2847E - 02	65.7267	1.5595	1.5288E - 03	7.3694E - 02	1.1088E - 02	1.7064E - 02	7
EO	0.7610	2.7768E - 07	3.6976E - 02	48.6793	1.4661	8.0049E - 04	2.7707E - 03	1.6102E - 03	5.4617E - 04	2
WOA	0.7621	2.6169E - 06	2.5104E - 02	94.3061	1.7276	4.1479E - 03	7.3695E - 02	2.4265E - 02	2.5528E - 02	8
GTO	0.7600	3.1068E - 07	3.6547E - 02	52.8898	1.4773	<b>7.7301E - 04</b>	9.5190E - 04	7.9298E - 04	4.4822E - 05	4
MPA	0.7605	8.3539E - 07	3.2009E - 02	93.8600	1.5835	1.7917E - 03	6.5239E - 03	4.0949E - 03	1.0978E - 03	3
SCA	0.7566	4.9527E - 08	3.9812E - 02	23.7660	1.3140	6.8097E - 03	2.1159E - 02	1.7709E - 02	4.4419E - 03	5
GWO	0.7612	1.1174E - 06	3.0709E - 02	91.3205	1.6179	2.3411E - 03	7.3696E - 02	1.7633E - 02	1.9719E - 02	6
SWO	<b>0.7608</b>	<b>3.1068E - 07</b>	<b>3.6547E - 02</b>	<b>52.8898</b>	<b>1.4773</b>	<b>7.7300E - 04</b>	<b>7.7300E - 04</b>	<b>7.7300E - 04</b>	<b>1.1055E - 17</b>	<b>1</b>

Bold values indicate the best results

$$I_D = I_{sd} \left( \exp \left( \frac{V + I * R_s}{n * V_t} \right) - 1 \right)$$

where  $I_{sd}$  indicates the reverse saturation current of this diode,  $R_s$  indicates the series resistance,  $V$  represents the output voltage,  $n$  is the factor of diode ideality, and  $V_t$  is modeled as follows:

$$V_t = \frac{k * T}{q}$$

where  $T$  is the junction's temperature in Kelvin,  $k$  is the Boltzmann constant ( $1.3806503 \times 10^{-23}$  J/K),  $q$  is the definition of electron charge and equal to  $1.60217646 \times 10^{-19}$  C, and  $I_{sh}$  is the shunt resistor current and calculated utilizing the formula:

$$I_{sh} = \frac{V + I * R_s}{R_{sh}}$$

where  $R_{sh}$  is shunt resistance.  $I$  is reformulated as follows:

$$I = I_{ph} - I_{sd} \left( \exp \left( \frac{q * (V + I * R_s)}{n * k * T} \right) - 1 \right) - \frac{V + I * R_s}{R_{sh}}$$

According to the previous description, five unknown parameters, namely,  $I_{ph}$ ,  $I_{sd}$ ,  $n$ ,  $R_s$ , and  $R_{sh}$ , have to be accurately estimated to accurately and effectively simulate the SDM.

The proposed and rival methods are validated on the parameter estimation problem of the SDM to determine the most effective one in finding the values of the near-optimal parameters that minimize RMSE between the measured and the estimated values. At the outset, all algorithms have been executed 25 times, and the fitness values obtained within these independent runs are analyzed and reported in Table 13. This table reveals the effectiveness of SWO because it could occupy the first rank compared with to all rival methods. Figure 21a and b compare the SWO and rival methods in terms of convergence curve and five-number summary. The figures demonstrate that SWO is the best compared with all the others. Figure 21c and d picture the I-V and

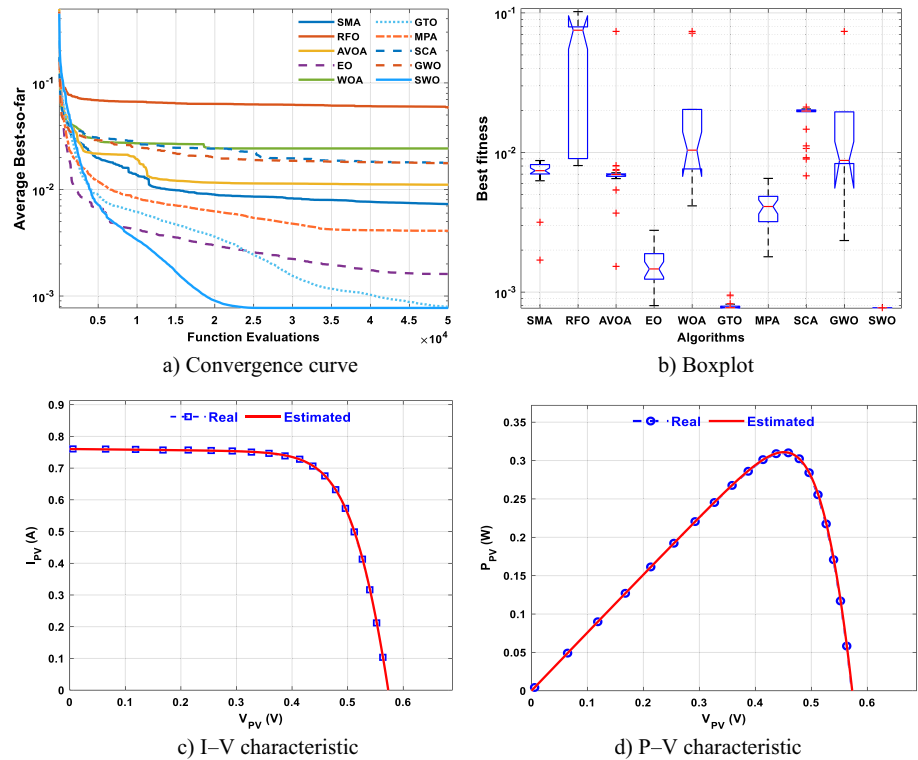


**Fig. 21** Various comparisons on SDM

P–V measured and estimated values, respectively. The figures are consistent between the measured and the estimated data.

### 5.3.2 DDM

The DDM output is computed according to the following formula:

$$I = I_{ph} - I_{D1} - I_{D2} - I_{sh}$$

where  $I$  can be substituted by the following detailed formula:

$$I = I_{ph} - I_{sd1} \left( \exp \left( \frac{V + I * R_s}{n_1 * V_t} \right) - 1 \right) - I_{sd2} \left( \exp \left( \frac{V + I * R_s}{n_2 * V_t} \right) - 1 \right) - \frac{V + I * R_s}{R_{sh}}$$

where  $I_{sd1}$  refers to the first diode current, and  $I_{sd2}$  stands for the second diode currents; and  $n_1$  and  $n_2$  stand for the diodes' ideality factors. However, seven parameters in this formula, namely,  $I_{ph}$ ,  $I_{sd1}$ ,  $I_{sd2}$ ,  $R_s$ ,  $R_{sh}$ ,  $n_1$ , and  $n_2$ , are not given in the manufacturing sheet, and the DDM could be accurately simulated without these parameters. In this section, we try to estimate the near-optimal values under the proposed algorithm and rival ones to determine the one that could optimally tackle this problem. Table 14 reports the outcomes obtained by each algorithm. This table illustrates the superiority of the suggested overall compared

**Table 14** Results of DDM compared with the rival methods

Algorithms	Best-obtained parameters				RMSE				Rank
	$I_{ph}(A)$	$I_{sd1}(A)$	$I_{sd2}(A)$	$R_s(\Omega)$	$R_{sh}(\Omega)$	$n_1$	$n_2$	Worst	
SMA	0.78291	3.237E-06	3.352E-06	0.17342	238.58322	1.82798	1.82790	1.404E-01	3.846E-01
RFO	0.75890	1.000E-09	5.000E-06	0.04269	480.30023	1.08927	1.97008	1.678E-03	1.979E-01
AVOA	0.76083	1.000E-09	3.761E-07	0.03703	53.50529	1.18793	1.50946	7.659E-04	6.945E-02
EO	0.76078	7.582E-08	8.060E-07	0.03747	56.27577	1.37290	1.75400	7.464E-04	2.868E-03
WOA	0.76021	1.000E-09	3.109E-06	0.04073	246.44413	1.09998	1.85162	1.812E-03	7.083E-02
GTO	0.76080	8.595E-08	9.996E-07	0.03764	56.25731	1.37802	1.81865	7.421E-04	7.508E-02
MFA	0.75963	1.042E-09	4.960E-06	0.04449	151.60023	1.08675	1.99501	1.498E-03	1.267E-02
SCA	0.75789	5.689E-09	8.674E-07	0.04018	90.60402	1.22996	1.64113	5.023E-03	1.963E-02
GWO	0.76008	7.093E-08	1.659E-06	0.03960	66.49396	1.25415	1.96988	1.122E-03	6.967E-02
SWO	<b>0.76081</b>	<b>8.945E-08</b>	<b>2.117E-06</b>	<b>0.03799</b>	<b>58.22408</b>	<b>1.37534</b>	<b>2.00000</b>	<b>7.327E-04</b>	<b>7.729E-04</b>
									<b>7.422E-04</b>

Bold values indicate the best results

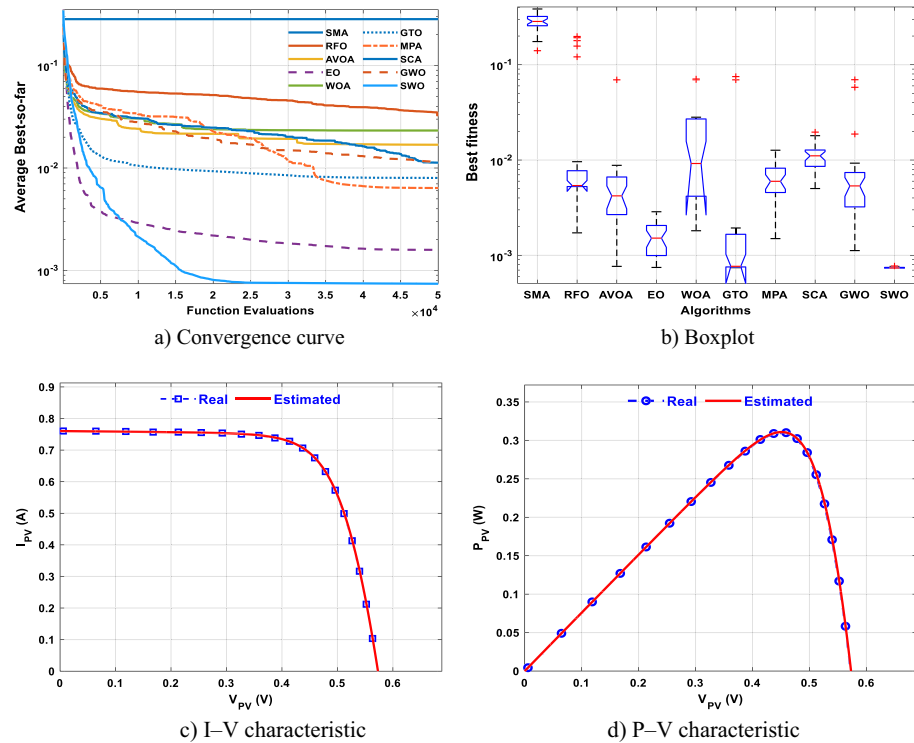


**Fig. 22** Various comparisons on DDM

ones. Figure 22 depicts the convergence curve in Fig. 22a, boxplot in Fig. 22b, harmonization between the P–V measured and estimated values in Fig. 22c, and the harmonization between the I–V measured and estimated values in Fig. 22c. Those figures affirm the effectiveness of the suggested algorithm.

### 5.3.3 TDM

The TDM consists of a photo-current source ( $I_{ph}$ ), three diodes connected in parallel, a series resistance ( $R_s$ ), and a shunt resistor ( $R_{sh}$ ). The output current of TDM is computed according to the following formula:

$$I = I_{ph} - \sum_i^3 I_{Di} - I_{sh}$$

where  $I_{ph}$   $I_{ph}$  indicates the photo-current source,  $I_{Di}$  denotes the current in the  $i^{th}$  diode (Fossum and Lindholm 1980; Koohi-Kamali et al. 2016), and  $I_{Di}$  and  $I_{sh}$  can be computed according to the following:

$$I_{Di} = I_{sdi} \left( e^{\frac{V+IR_s}{a_i V_t}} - 1 \right), \forall i \in 1 : 3, V_t = \frac{KT}{q}$$

$$I_{sh} = \frac{V + IR_s}{R_{sh}}$$

where  $I_{sd_i}$  stands for the  $i$ th diode saturation current,  $V$  indicates the output voltage of the cell,  $a_i$  refers to the ideality factor of the  $i$ th diode,  $R_s$  is the series resistance,  $K$  is the Boltzmann's constant and equal to  $1.3806503 * 10^{-23}\text{J/K}$ ,  $q$  is the electron charge with a constant value of  $1.60217646 * 10^{-19}\text{C}$ , and  $T$  is the cell temperature in kelvin (K). The previous description elaborates that the mathematical model of TDM contains nine unknown parameters ( $I_{ph}, I_{sd1}, I_{sd2}, I_{sd3}, R_s, R_{sh}, a_1, a_2$ , and  $a_3$ ) that have to be accurately identified for simulating the TDM. This section presents the outcomes (Table 15) of testing the performance of SWO for estimating those unknown parameters in addition to making extensive comparisons with the outcomes of the rival algorithms to demonstrate the effectiveness of our proposed algorithm to the readers. Table 15 presents the best-extracted parameters by each algorithm in addition to reporting the analysis outcomes of the fitness values across 25 independent runs. This table reveals that SWO is the best because it could overcome all the algorithms. Figure 23 presents the averaged convergence curve, five-number summary (Boxplot), consistency between the I-V measured and current values, and consistency between the P-V measured and current values. This figure demonstrates that SWO performs better for this problem.

#### 5.4 Wilcoxon rank-sum test

Table 15 illustrates the p-values obtained by applying the Wilcoxon rank-sum analysis test on the outcomes of SWO with those of each competitor for five-investigated real-world problems, namely, WBD, PVD, SDM, DDM, and TDM. The outcomes of SWO compared with the other algorithms are significantly different because the p-values for all test cases and rival algorithms are less than the accuracy level of 5%.

## 6 The overall effectiveness of SWO: key findings

The previous sections have examined SWO's performance on four benchmarks (CEC2005, CEC2014, CEC2017, and CEC2020) and five real-world optimization issues, in addition to comparing to some state-of-the-arts. However, the key findings of SWO across all test suites still require elaboration. Thus, this section contrasts SWO's total performance with that of the other algorithms over all test functions of each benchmark. Table 17 compares the proposed algorithm to its competitors in terms of their success rate (SP) using an extra parameter called overall effectiveness (OE), which is computed using the following formula (Nadimi-Shahraki and Zamani 2022):

$$\text{OE}(\%) = \frac{N' - L_i}{N'} * 100$$

where  $N'$  is the number of mathematical functions in the test suite;  $L_i$  is the number of test functions, which an algorithm performed poorly compared to the other optimizers. According to the findings in this table, SWO could have better OE for four test suites and five real-world problems with percentages up to 78.2% for CEC2005, 92.31% for CEC2014,

**Table 15** Results of TDM compared with the rival methods

Algorithms	Best-obtained parameters						RMSE							
	$I_{ph}(A)$	$I_{sd1}(A)$	$I_{sd2}(A)$	$I_{sd3}(A)$	$R_c(Q)$	$R_{sh}(Q)$	$n_1$	$n_2$	$n_3$	Best	Worst	Ave	Std	
SMA	0.761	5.14E - 06	6.79E - 09	1.99E - 09	0.040	108.887	2.000	1.200	1.878	1.1903E - 03	6.436E - 03	2.779E - 03	1.092E - 03	10
RFO	0.761	1.00E - 09	1.00E - 05	1.00E - 09	0.029	474.828	1.126	2.000	1.784	5.6335E - 03	1.882E - 02	8.224E - 03	2.195E - 03	9
AVOA	0.760	3.07E - 06	1.65E - 09	8.67E - 08	0.037	88.812	1.994	1.200	1.400	1.0220E - 03	6.282E - 03	3.645E - 03	1.540E - 03	7
EO	0.760	7.89E - 07	1.17E - 07	1.44E - 07	0.034	129.168	1.670	1.445	1.917	1.6260E - 03	4.424E - 03	2.600E - 03	6.382E - 04	2
WOA	0.760	1.45E - 09	1.14E - 09	5.38E - 07	0.035	93.627	1.380	1.267	1.540	1.2635E - 03	8.696E - 03	6.161E - 03	2.244E - 03	8
GTO	0.761	1.00E - 09	8.36E - 08	2.22E - 06	0.038	61.621	2.000	1.370	2.000	7.5091E - 04	2.773E - 03	9.794E - 04	4.873E - 04	4
MPA	0.760	3.16E - 07	1.00E - 09	4.27E - 07	0.037	65.420	1.492	1.204	2.000	9.7914E - 04	4.416E - 03	2.372E - 03	8.143E - 04	3
SCA	0.761	2.30E - 09	3.04E - 09	2.66E - 07	0.039	65.054	1.875	2.000	1.461	2.4019E - 03	6.636E - 03	3.847E - 03	9.700E - 04	5
GWO	0.761	1.99E - 06	6.98E - 09	1.19E - 07	0.037	63.395	2.000	1.749	1.400	7.8399E - 04	5.510E - 03	2.668E - 03	1.155E - 03	6
SWO	<b>0.760</b>	<b>3.55E - 07</b>	<b>9.37E - 08</b>	<b>1.70E - 06</b>	<b>0.038</b>	<b>61.165</b>	<b>2.000</b>	<b>1.379</b>	<b>1.995</b>	<b>7.5085E - 04</b>	<b>7.863E - 04</b>	<b>7.648E - 04</b>	<b>9.762E - 06</b>	<b>1</b>

Bold values indicate the best results

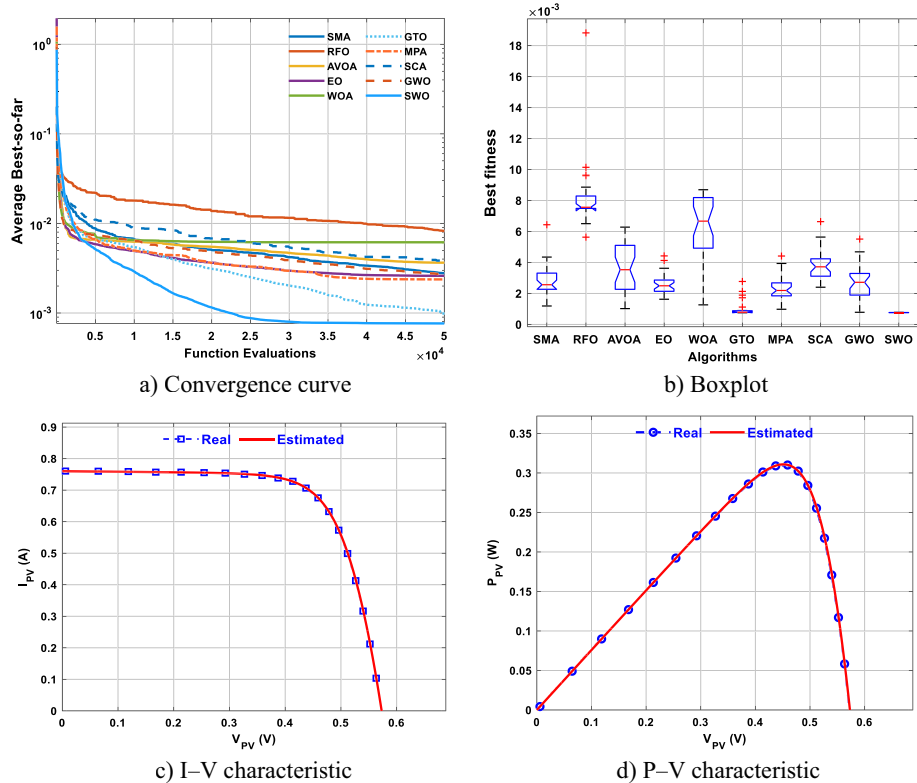


**Fig. 23** Various comparisons on TDM

77.78% for CEC2017, 60% for CEC2020, and 100% for real-world problems. Our key findings after all validation and comparison conducted in this study are as follows:

- SWO belongs to the category of high-performance optimizer due to its strong performance for a wide range of optimization problems, especially real-world optimization problems.
- Designing a newly-proposed meta-heuristic algorithm with several effective controlling parameters consider is an advantage because it will make it relevant to a variety of optimization problems with different requirements.
- The only disadvantage of SWO is reaching the values of the control parameters that maximize its performance.

## 7 Conclusion and future perspective

This work presents a new nature-inspired swarm-based meta-heuristic algorithm, namely, spider wasp optimizer (SWO), inspired by hunting, nesting, and mating behaviors of the female spider wasps in nature. The proposed SWO consists four stages that imitate

**Table 16** p-Values of the Wilcoxon rank-sum test for five-investigated real-world problems

	SMA	RFO	AVOA	EO	WOA	GTO	MPA	SCA	GWO
WBD	p-value	1.2100E-12	1.2100E-12	1.2100E-12	1.2100E-12	4.5700E-12	1.2100E-12	1.2100E-12	1.2100E-12
	<i>h</i>	1	1	1	1	1	1	1	1
PWD	p-value	1.7200E-12							
	<i>h</i>	1	1	1	1	1	1	1	1
SDM	p-value	3.0180E-	3.0180E-11						
	<i>h</i>	1	1	1	1	1	1	1	1
DDM	p-value	3.0200E-11	3.0200E-11	3.3380E-11	6.6960E-11	3.0200E-11	3.6460E-08	3.0200E-11	3.0200E-11
	<i>h</i>	1	1	1	1	1	1	1	1
TDM	p-value	3.0200E-11	3.0200E-11	3.0200E-11	3.0200E-11	3.8310E-05	3.0200E-11	3.0200E-11	3.6900E-11
	<i>h</i>	1	1	1	1	1	1	1	1

**Table 17** Key findings/overall effectiveness of SWO

Benchmarks	SMA (%)	RFO (%)	AVOA (%)	EO (%)	WOA (%)	GTO (%)	MPA (%)	SCA (%)	GWO (%)	SWO (%)
CEC2005	65.22	65.22	73.91	43.48	47.83	69.57	43.48	21.74	39.13	<b>78.26</b>
CEC2014	0.00	0.00	0.00	0.00	0.00	0.00	23.08	0.00	0.00	<b>92.31</b>
CEC2017	0.00	0.00	5.56	5.56	0.00	11.11	33.33	0.00	0.00	<b>77.78</b>
CEC2020	10.00	30.00	10.00	0.00	0.00	10.00	30.00	0.00	0.00	<b>60.00</b>
Real-world	0.00	0.00	0.00	0.00	0.00	0.00	0.00	0.00	0.00	<b>100.00</b>

Bold values indicate the best outcomes

0.00% means that the algorithm could not be the best for any test function

searching for the spider, following and escaping dropped spider, nesting the paralyzed spider, and mating behavior of the female spider wasps to lay an egg. Four different benchmarks were extensively employed to analyze the exploitation, exploration, escaping from local optima, and convergence speed of the proposed SWO. The proposed SWO outperformed nine state-of-art optimization algorithms over those benchmarks.

Two classical engineering design problems, namely, WBD and pressure vessel design, and the parameter identification of SDM, DDM, and TDM were tackled to further validate the performance of SWO. The experimental findings of those problems proved that SWO was superior compared with nine well-established and newly published state-of-art metaheuristic algorithms: SMA, MPA, EO, GTO, AVOA, GWO, WOA, SCA, and RFO. Our future work involves developing binary and multi-objective versions of SWO.

## Appendix A

See Table 18.

**Table 18** Description of some standard test functions

Functions	D	Domain	Global opt
$F1 = \sum_{i=1}^D x_i^2$	50	[-100,100]	0
$F2 = \sum_{i=1}^D  x_i  + \prod_{i=1}^D  x_i $	50	[-100,100]	0
$F3 = \sum_{i=1}^D \left( \sum_{j=1}^D x_j \right)^2$	50	[-100,100]	0
$F4 = \max\{ x_i \}  1 \leq i \leq D$	50	[-100,100]	0
$F5 = \sum_{i=1}^{D-1} \left[ 100(x_{i+1} - x_i^2)^2 + (x_i - 1)^2 \right]$	50	[-30,30]	0
$F6 = \sum_{i=1}^{D-1} [x_i + 0.5]^2$	50	[-100,100]	0
$F7 = \sum_{i=1}^D i x_i^4 + \text{random}[0,1]$	50	[-1.28,1.28]	0
$F8 = \sum_{i=1}^{D-1} -x_i \sin\left(\sqrt{ x_i }\right)$	50	[-500,500]	-418.98 $\times D$
$F9 = \sum_{i=1}^D [x_i^2 - 10\cos(2\pi x_i) + 10]$	50	[-5.12,5.12]	0
$F10 = -20\exp\left(-0.2\sqrt{\frac{1}{D} \sum_{i=1}^D x_i^2}\right) - \exp\left(\frac{1}{D} \sum_{i=1}^D \cos(2\pi x_i)\right) + 20 + e$	50	[-32,32]	0
$F11 = \frac{1}{400} \sum_{i=1}^D x_i^2 - \prod_{i=1}^D \cos\left(\frac{x_i}{\sqrt{i}}\right) + 1$	50	[-600,600]	0
$F12 = \frac{\pi}{D} \{10\sin(\pi y_1) + \sum_{i=1}^{D-1} (y_i - 1)^2 [1 + 10\sin^2(\pi y_{i+1})]\} + (y_D - 1)^2 \} + \sum_{i=1}^D u(x_i, 10, 100, 4)$	50	[-50,50]	0
$F13 = \frac{\pi}{d} \{10\sin^2(3x_1) + \sum_{i=1}^{D-1} (x_i - 1)^2 [1 + \sin^2(3\pi x_i)] + (x_d - 1)^2 [1 + \sin^2(2\pi x_D)]\} + \sum_{i=1}^d u(x_i, 5, 100, 4)$	50	[-50,50]	0
$F14 = \left( \frac{1}{500} + \sum_{j=1}^{25} \frac{1}{j + \sum_{i=1}^j (x_i - a_{ij})^2} \right)^{-1}$	2	[-65,65]	1

See Fig. 24.

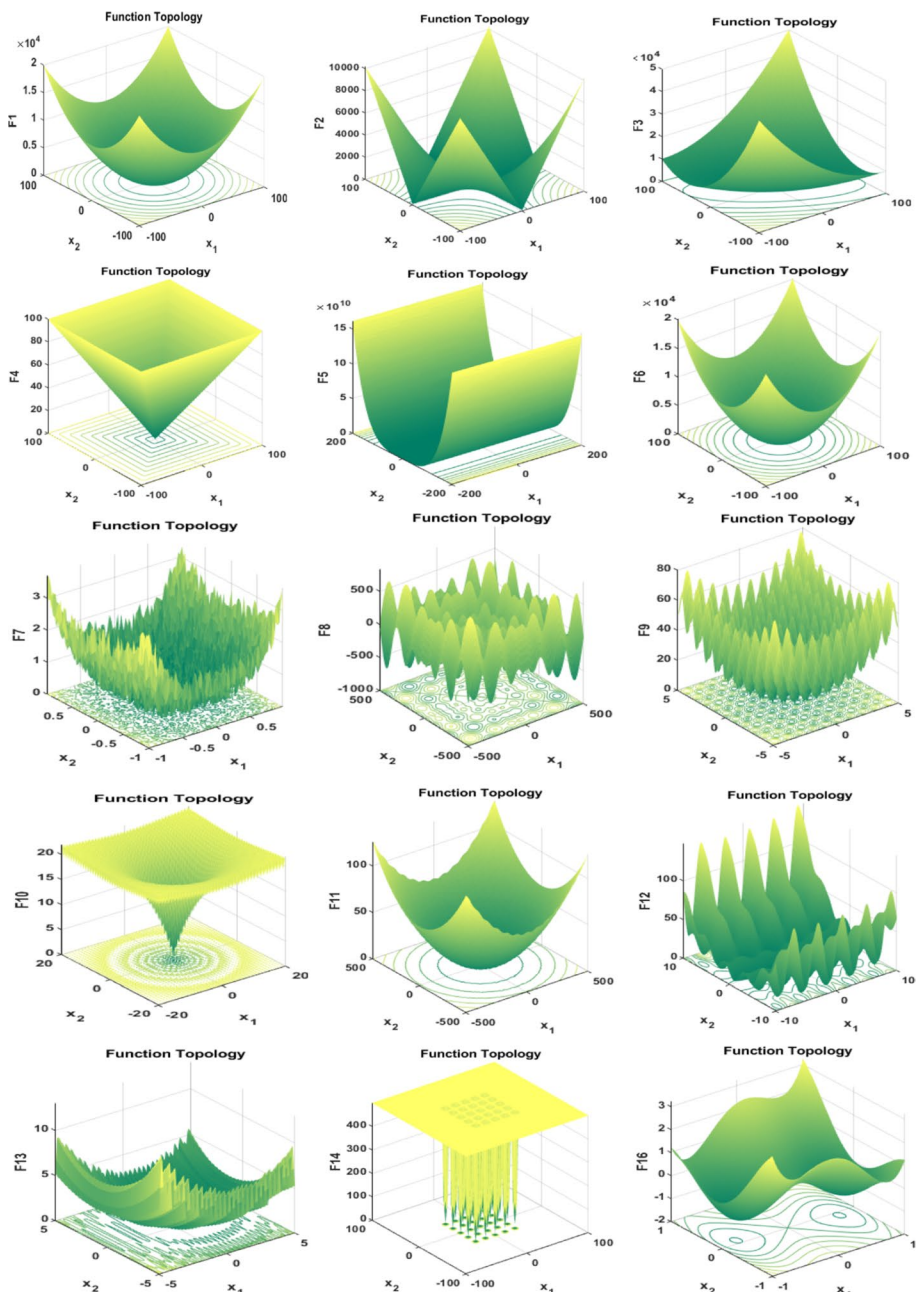


**Fig. 24** Topologies of some mathematical test functions in standard benchmark

See Tables 19, 20, 21.

**Table 19** Properties of 18 CEC-2017 test functions

Type	ID	Functions	Global opt	Domain
Unimodal function	F24 (CF1)	Function of shifted and rotated bent cigar	100	[−100, 100]
	F25 (CF3)	Function of shifted and rotated Zakharov	300	[−100, 100]
Simple multimodal Test functions	F26 (CF5)	Shifted and rotated Rastrigin's function	500	[−100, 100]
	F27 (CF6)	Shifted and rotated expanded Scaffer's function	600	[−100, 100]
	F28 (CF7)	Shifted and rotated Lunacek Bi_Rastrigin function	700	[−100, 100]
	F29 (CF8)	Shifted and rotated non-continuous Rastrigin's function	800	[−100, 100]
	F30 (CF9)	Shifted and rotated levy function	900	[−100, 100]
Hybrid test functions	F31 (CF14)	Function 4 hybrid	1400	[−100, 100]
	F32 (CF17)	Function 7 hybrid	1700	[−100, 100]
	F33 (CF18)	Function 8 hybrid	1800	[−100, 100]
	F34 (CF19)	Function 9 hybrid	1900	[−100, 100]
	F35 (CF20)	Function 10 hybrid	2000	[−100, 100]
Composition test functions	F36 (CF21)	Function 1 composition	2100	[−100, 100]
	F37 (CF22)	Function 2 composition	2200	[−100, 100]
	F38 (CF23)	Function 3 composition	2300	[−100, 100]
	F39 (CF24)	Function 4 composition	2400	[−100, 100]
	F40 (CF26)	Function 6 composition	2600	[−100, 100]
	F41 (CF28)	Function 8 composition	2800	[−100, 100]

**Table 20** Properties of 13 CEC-2014 test functions

Type	ID	Functions	Global opt	Domain
Unimodal function	F42 (CF2)	Function of rotated bent cigar	200	[−100, 100]
	F43 (CF3)	Function of rotated discus	300	[−100, 100]
Simple multimodal test functions	F44 (CF4)	Shifted and Rotated Rosenbrock's function	400	[−100, 100]
	F45 (CF6)	Shifted and rotated Weierstrass function	600	[−100, 100]
	F46 (CF7)	Shifted and rotated Griewank's function	700	[−100, 100]
	F47 (CF8)	Shifted Rastrigin's function	800	[−100, 100]
	F48 (CF9)	Shifted and rotated Rastrigin's function	900	[−100, 100]
	F49 (CF10)	Shifted Schwefel's function	1000	[−100, 100]
Hybrid test functions	F50 (CF19)	Function 3 hybrid	1900	[−100, 100]
	F51 (CF21)	Function 5 hybrid	2100	[−100, 100]
	F52 (CF22)	Function 6 hybrid	2100	[−100, 100]
Composition test functions	F53 (CF23)	Function 1 composition	2300	[−100, 100]
	F54 (CF27)	Function 5 composition	2700	[−100, 100]

**Table 21** Characteristics of CEC-2020 test functions

Type	ID	Functions	Global opt	Domain
Unimodal	F83 (CF1)	Shifted and rotated bent cigar function	100	[− 100, 100]
Multimodal	F84 (CF2)	Shifted and rotated Lunacek Bi_Rastrigin function	700	[− 100, 100]
Hybrid test functions	F85 (CF3)	Function 1 hybrid	1100	[− 100, 100]
	F86 (CF4)	Function 2 hybrid	1700	[− 100, 100]
	F87 (CF5)	Function 3 hybrid	1900	[− 100, 100]
	F88 (CF6)	Function 4 hybrid	2100	[− 100, 100]
	F89 (CF7)	Function 5 hybrid	1600	[− 100, 100]
Hybrid test functions	F90 (CF8)	Function 1 composition	2200	[− 100, 100]
	F91 (CF9)	Function 2 composition	2400	[− 100, 100]
	F92 (CF10)	Function 3 composition	2500	[− 100, 100]

## References

- Abdollahzadeh B, Soleimanian Gharehchopogh F, Mirjalili S (2021a) Artificial gorilla troops optimizer: a new nature-inspired metaheuristic algorithm for global optimization problems. *Int J Intell Syst* 36(10):5887–5958
- Abdollahzadeh B, Gharehchopogh FS, Mirjalili S (2021b) African vultures optimization algorithm: a new nature-inspired metaheuristic algorithm for global optimization problems. *Comput Ind Eng* 158:107408
- Aguiar AP et al (2013) Order Hymenoptera, In: Zhang, Z.Q. (Ed.) Animal biodiversity: an outline of higher-level classification and survey of taxonomic richness (Addenda 2013). *Zootaxa* 3703(1):51–62
- Alavi M, Henderson JC (1981) An evolutionary strategy for implementing a decision support system. *Manage Sci* 27(11):1309–1323
- Askari Q, Younas I, Saeed M (2020) Political Optimizer: A novel socio-inspired meta-heuristic for global optimization. *Knowl-Based Syst* 195:105709
- Auko T, Silvestre R, Pitts J (2013) Nest camouflage in the spider wasp *Priocnemis captivum* (Fabricius, 1804) (Hymenoptera: Pompilidae), with notes on the biology. *Trop Zool* 26(3):140–144
- Awad NH, Ali MZ, Suganthan PN (2017) Ensemble sinusoidal differential covariance matrix adaptation with Euclidean neighborhood for solving CEC2017 benchmark problems. 2017 IEEE congress on evolutionary computation (CEC). IEEE
- Benamu M et al (2020) Koinobint life style of the spider wasp *Minagenia* (Hymenoptera, Pompilidae) and its consequences for host selection and sex allocation. *Zoology* 140:125797
- Bianchi L et al (2009) A survey on metaheuristics for stochastic combinatorial optimization. *Nat Comput* 8:239–287
- Birbil Şİ, Fang SC (2003) An electromagnetism-like mechanism for global optimization. *J Global Optim* 25(3):263–282
- Bodaghi M, Samieefar K (2019) Meta-heuristic bus transportation algorithm. *Iran J Comput Sci* 2:23–32
- Bołaji ALA et al (2016) A comprehensive review: Krill Herd algorithm (KH) and its applications. *Appl Soft Comput* 49:437–446
- Carvalho-Filho FDS, Auko TH, Waichert C (2015) Observations on the nesting behaviour of the spider wasp *Ergenias congrua* (Hymenoptera: Pompilidae), with the first record of the host. *J Nat Hist* 49(33–34):2035–2044
- Charnov EL et al (1981) Sex ratio evolution in a variable environment. *Nature* 289(5793):27–33
- Chen X et al (2018) Teaching–learning–based artificial bee colony for solar photovoltaic parameter estimation. *Appl Energy* 212:1578–1588
- Chou J-S, Truong D-N (2021) A novel metaheuristic optimizer inspired by behavior of jellyfish in ocean. *Appl Math Comput* 389:125535
- Chu SC, Tsai PW, Pan JS (2006) Cat swarm optimization. Pacific Rim International Conference on Artificial Intelligence. Springer

- Chuang CL, Jiang JA (2007) Integrated radiation optimization: inspired by the gravitational radiation in the curvature of space-time. 2007 IEEE congress on evolutionary computation. IEEE
- Dorigo M, Birattari M, Stutzle T (2006) Ant colony optimization. *IEEE Comput Intell Mag* 1(4):28–39
- Du H, Wu X, Zhuang J (2006) Small-world optimization algorithm for function optimization. International conference on natural computation. Springer
- Easwarakhanthan T et al (1986) Nonlinear minimization algorithm for determining the solar cell parameters with microcomputers. *Int J Solar Energy* 4(1):1–12
- Endo T, Endo A (1994) Prey selection by a spider wasp, *Batozonellus lacerticida* (Hymenoptera: Pompilidae): effects of seasonal variation in prey species, size and density. *Ecol Res* 9:225–235
- Erol OK, Eksin I (2006) A new optimization method: big bang–big crunch. *Adv Eng Softw* 37(2):106–111
- Evans H, Shimizu A (1996) The evolution of nest building and communal nesting in *Ageniellini* (Insecta: Hymenoptera: Pompilidae). *J Nat Hist* 30(11):1633–1648
- Faramarzi A et al (2020a) Equilibrium optimizer: a novel optimization algorithm. *Knowl-Based Syst* 191:105190
- Faramarzi A et al (2020b) Marine predators algorithm: a nature-inspired metaheuristic. *Expert Syst Appl* 152:113377
- Flores JJ, López R, Barrera J (2011) Gravitational interactions optimization. Learning and intelligent optimization: 5th international conference, LION 5, Rome, Italy, January 17–21, 2011 selected papers 5. Springer
- Formato RA (2007) Central force optimization. *Prog Electromagn Res* 77(1):425–491
- Fossum JG, Lindholm FA (1980) Theory of grain-boundary and intragrain recombination currents in polysilicon pn-junction solar cells. *IEEE Trans Electron Devices* 27(4):692–700
- Gandomi AH, Yang X-S, Alavi AH (2013) Cuckoo search algorithm: a metaheuristic approach to solve structural optimization problems. *Eng Comput* 29(1):17–35
- Ghorbani N, Babaei E (2014) Exchange market algorithm. *Appl Soft Comput* 19:177–187
- Glover FW, Kochenberger GA (2006) Handbook of metaheuristics, vol 57. Springer Science & Business Media
- Gong W, Cai Z (2013) Parameter extraction of solar cell models using repaired adaptive differential evolution. *Sol Energy* 94:209–220
- Grissell E (1997) The hymenoptera of costa rica. Oxford University Press, Oxford
- Hashim FA et al (2019) Henry gas solubility optimization: a novel physics-based algorithm. *Futur Gener Comput Syst* 101:646–667
- Holland JH (1992) Genetic algorithms. *Sci Am* 267(1):66–73
- Hsiao YT et al (2005) A novel optimization algorithm: space gravitational optimization. 2005 IEEE international conference on systems, man and cybernetics. IEEE
- Javidy B, Hatamlou A, Mirjalili S (2015) Ions motion algorithm for solving optimization problems. *Appl Soft Comput* 32:72–79
- Kaveh A, Khayatiazad M (2012) A new meta-heuristic method: ray optimization. *Comput Struct* 112:283–294
- Kaveh A, Talatahari S (2010) A novel heuristic optimization method: charged system search. *Acta Mech* 213(3):267–289
- Kennedy J, Eberhart R (1995) Particle swarm optimization. Proceedings of ICNN'95-international conference on neural networks. IEEE
- King BH (1988) Sex-ratio manipulation in response to host size by the parasitoid wasp *Spalangia cameroni*: a laboratory study. *Evolution* 42(6):1190–1198
- Kirkpatrick S, Gelatt CD Jr, Vecchi MP (1983) Optimization by simulated annealing. *Science* 220(4598):671–680
- Koohi-Kamali S et al (2016) Photovoltaic electricity generator dynamic modeling methods for smart grid applications: a review. *Renew Sustain Energy Rev* 57:131–172
- Koza JR, Koza JR (1992) Genetic programming: on the programming of computers by means of natural selection, vol 1. MIT press
- Kumar M, Kulkarni AJ, Satapathy SC (2018) Socio evolution & learning optimization algorithm: a socio-inspired optimization methodology. *Future Gener Comput Syst* 81:252–272
- Kurczewski FE, Edwards G (2012) Hosts, nesting behavior, and ecology of some North American spider wasps (Hymenoptera: Pompilidae). *Southeast Nat* 11(m4):1–71
- Kurczewski FE, Kiernan DH (2015) Analysis of spider wasp host selection in the eastern Great Lakes Region (Hymenoptera: Pompilidae). *Northeast Nat* 22(m11):1–88
- Li S et al (2019) Parameter extraction of photovoltaic models using an improved teaching-learning-based optimization. *Energy Convers Manage* 186:293–305

- Li S et al (2020) Slime mould algorithm: a new method for stochastic optimization. *Futur Gener Comput Syst* 111:300–323
- Loktionov V, Lelej A, Liu J-X (2019) A new genus of spider wasps (Hymenoptera, Pompilidae) from China. *Far Eastern Entomol* 376:1–14
- Meng X et al (2014) A new bio-inspired algorithm: chicken swarm optimization. International Conference in Swarm Intelligence. Springer
- MiarNaeimi F, Azizyan G, Rashki M (2021) Horse herd optimization algorithm: a nature-inspired algorithm for high-dimensional optimization problems. *Knowl-Based Syst* 213:106711
- Mirjalili S (2016) SCA: a sine cosine algorithm for solving optimization problems. *Knowl-Based Syst* 96:120–133
- Mirjalili S, Lewis A (2016) The whale optimization algorithm. *Adv Eng Softw* 95:51–67
- Mirjalili S, Mirjalili SM, Lewis A (2014) Grey wolf optimizer. *Adv Eng Softw* 69:46–61
- Mirjalili S, Mirjalili SM, Hatamlou A (2016) Multi-verse optimizer: a nature-inspired algorithm for global optimization. *Neural Comput Appl* 27(2):495–513
- Mirjalili S et al (2017) Salp swarm algorithm: a bio-inspired optimizer for engineering design problems. *Adv Eng Softw* 114:163–191
- Moghaddam FF, Moghaddam RF, Cheriet M (2012) Curved space optimization: a random search based on general relativity theory. Cornell University
- Moosavian N, Roodsari BK (2014) Soccer league competition algorithm: a novel meta-heuristic algorithm for optimal design of water distribution networks. *Swarm Evol Comput* 17:14–24
- Nadimi-Shahraki MH, Zamani H (2022) DMDE: diversity-maintained multi-trial vector differential evolution algorithm for non-decomposition large-scale global optimization. *Expert Syst Appl* 198:116895
- Naik A, Satapathy SC (2021) Past present future: a new human-based algorithm for stochastic optimization. *Soft Comput* 25(20):12915–12976
- Nieves-Aldrey J, Fontal-Cazalla F, Fernández F (2006) Introducción a los Hymenoptera de la Región Neotropical. Universidad Nacional de Colombia
- Nishimoto Y et al (2021) Life history and nesting ecology of a Japanese tube-nesting spider wasp *Dipogon sperconsus* (Hymenoptera: Pompilidae). *Sci Rep* 11(1):1–11
- Nunes H et al (2018) A new high performance method for determining the parameters of PV cells and modules based on guaranteed convergence particle swarm optimization. *Appl Energy* 211:774–791
- Opp SB, Luck RF (1986) Effects of host size on selected fitness components of *Aphytis melinus* and *A. lingnanensis* (Hymenoptera: Aphelinidae). *Ann Entomol Soc Am* 79(4):700–704
- Pinto PC, Runkler TA, Sousa JM (2007) Wasp swarm algorithm for dynamic MAX-SAT problems. International conference on adaptive and natural computing algorithms. Springer
- Pitts JP, Wasbauer MS, Von Dohlen CD (2006) Preliminary morphological analysis of relationships between the spider wasp subfamilies (Hymenoptera: Pompilidae): revisiting an old problem. *Zoolog Scr* 35(1):63–84
- Połap D, Woźniak M (2021) Red fox optimization algorithm. *Expert Syst Appl* 166:114107
- Price KV (2013) Differential evolution. Handbook of optimization. Springer, pp 187–214
- Punzo F (1994) The biology of the spider wasp *Pepsis thisbe* (Hymenoptera: Pompilidae) from trans Pecos, Texas I adult morphometrics, larval development and the ontogeny of larval feeding patterns. *Psyche* 101(3–4):229–241
- Rabanal P, Rodríguez I, Rubio F (2007) Using river formation dynamics to design heuristic algorithms. International conference on unconventional computation. Springer
- Rao RV, Savsani VJ, Vakharia D (2011) Teaching–learning-based optimization: a novel method for constrained mechanical design optimization problems. *Comput Aided Des* 43(3):303–315
- Rayor LS (1996) Attack strategies of predatory wasps (Hymenoptera: Pompilidae; Sphecidae) on colonial orb web-building spiders (Araneida: Metepeira incrassata). *J Kansas Entomol Soc* 1996:67–75
- Sacco WF, Oliveira C (2005) A new stochastic optimization algorithm based on a particle collision metaheuristic. Proceedings of 6th WCSMO
- Sahab MG, Toropov VV, Gandomi AH (2013) A review on traditional and modern structural optimization: problems and techniques. Metaheuristic applications in structures and infrastructures. Elsevier, pp 25–47
- Shah-Hosseini H (2009) The intelligent water drops algorithm: a nature-inspired swarm-based optimization algorithm. *Int J Bio-Inspir Comput* 1(1–2):71–79
- Shah-Hosseini H (2011) Principal components analysis by the galaxy-based search algorithm: a novel metaheuristic for continuous optimisation. *Int J Comput Sci Eng* 6(1–2):132–140
- Shamsaldin AS et al (2019) Donkey and smuggler optimization algorithm: a collaborative working approach to path finding. *J Comput Design Eng* 6(4):562–583
- Shi Y (2011) Brain storm optimization algorithm. International conference in swarm intelligence. Springer

- Shimizu A (1992) Nesting behavior of the semi-aquatic spider wasp, *Anoplius eous*, which transports its prey on the surface film of water (Hymenoptera, Pompilidae). J Ethol 10(2):85–102
- Shimizu A, Wasbauer M, Takami Y (2010) Phylogeny and the evolution of nesting behaviour in the tribe Ageniellini (Insecta: Hymenoptera: Pompilidae). Zool J Linn Soc 160(1):88–117
- Shimizu A et al (2012) Brood parasitism in two species of spider wasps (Hymenoptera: Pompilidae, Dipogon), with notes on a novel reproductive strategy. J Insect Behavior 25:375–391
- Starr C (2012) Nesting biology and sex ratio in a Neotropical spider wasp, *Priocnemis captivum* (Hymenoptera: Pompilidae). Trop Zool 25(2):62–66
- Tan YT, Kirschen DS, Jenkins N (2004) A model of PV generation suitable for stability analysis. IEEE Trans Energy Convers 19(4):748–755
- Wahis R, Lelej A, Loktionov V (2018) Contribution to the knowledge of the genus *Eopompilus* Gussakovskij, 1932 (Hymenoptera, Pompilidae). Far Eastern Entomologist 361:1–11
- Waichert C et al (2015) Molecular phylogeny and systematics of spider wasps (Hymenoptera: Pompilidae): redefining subfamily boundaries and the origin of the family. Zool J Linn Soc 175(2):271–287
- Wang GG, Deb S, Coelho LDS (2015) Elephant herding optimization. 2015 3rd international symposium on computational and business intelligence (ISCBI). IEEE
- Webster B, Bernhard PJ (2003) A local search optimization algorithm based on natural principles of gravitation. Proceeding of the 2003 international conference on information and knowledge engineering (IKE'03). Florida Tech, USA, pp 23–26
- Xie L, Zeng J, Cui Z (2009) General framework of artificial physics optimization algorithm. 2009 world congress on nature & biologically inspired computing (NabIC). IEEE
- Yang XS (2012) Swarm-based metaheuristic algorithms and no-free-lunch theorems. Theory New Appl Swarm Intell 9:1–16
- Yang XS, Gandomi AH (2012) Bat algorithm: a novel approach for global engineering optimization. Eng Comput 2012:1–10
- Yang XS, Ting T, Karamanoglu M (2013) Random walks, Lévy flights, Markov chains and metaheuristic optimization. Future Info Commun Technol Appl ICFICE 2013:1055–1064
- Yao X, Liu Y, Lin G (1999) Evolutionary programming made faster. IEEE Trans Evol Comput 3(2):82–102
- Yu K et al (2017) Parameters identification of photovoltaic models using an improved JAYA optimization algorithm. Energy Convers Manage 150:742–753
- Yu K et al (2018) Multiple learning backtracking search algorithm for estimating parameters of photovoltaic models. Appl Energy 226:408–422

**Publisher's Note** Springer Nature remains neutral with regard to jurisdictional claims in published maps and institutional affiliations.

## Authors and Affiliations

Mohamed Abdel-Basset<sup>1</sup> · Reda Mohamed<sup>1</sup> · Mohammed Jameel<sup>2</sup> ·  
Mohamed Abouhawwash<sup>3,4</sup> 

Mohamed Abdel-Basset  
mohamedbasset@ieee.org

Reda Mohamed  
redamoh@zu.edu.eg

Mohammed Jameel  
moh.jameel@su.edu.ye; mohjameel555@gmail.com

<sup>1</sup> Faculty of Computers and Informatics, Zagazig University, Shaibet an Nakareyah, Zagazig 44519, Ash Sharqia Governorate, Egypt

<sup>2</sup> Department of Mathematics, Sana'a University, 13509 Sana'a, Yemen

<sup>3</sup> Department of Mathematics, Faculty of Science, Mansoura University, Mansoura 35516, Egypt

<sup>4</sup> Department of Computational Mathematics, Science, and Engineering (CMSE), Michigan State University, East Lansing, MI 48824, USA